Learning Memory-Enhanced Improvement Heuristics for Flexible Job Shop Scheduling

Jiaqi Wang[1,2], Zhiguang Cao[4], Peng Zhao[1,3]*, Rui Cao[1,3], Yubin Xiao[1,3], Yuan Jiang[5]*, You Zhou[1,2,3]*

[1]Key Laboratory of Symbolic Computation and Knowledge Engineering of Ministry of Education, Jilin University
[2]College of Software, Jilin University
[3]College of Computer Science and Technology, Jilin University
[4]Singapore Management University [5]Nanyang Technological University

{jqwang24, pengzhao23, ruicao24, xiaoyb21}@mails.jlu.edu.cn
zhiguangcao@outlook.com, yuan005@e.ntu.edu.sg, zyou@jlu.edu.cn

Abstract

The rise of smart manufacturing under Industry 4.0 introduces mass customization and dynamic production, demanding more advanced and flexible scheduling techniques. The flexible job-shop scheduling problem (FJSP) has attracted significant attention due to its complex constraints and strong alignment with real-world production scenarios. Current deep reinforcement learning (DRL)-based approaches to FJSP predominantly employ constructive methods. While effective, they often fall short of reaching (near-)optimal solutions. In contrast, improvement-based methods iteratively explore the neighborhood of initial solutions and are more effective in approaching optimality. However, the flexible machine allocation in FJSP poses significant challenges to the application of this framework, including accurate state representation, effective policy learning, and efficient search strategies. To address these challenges, this paper proposes a **M**emory-enhanced **I**mprovement **S**earch framework with he**t**erogeneous gr**a**ph **r**epresentation—*MIStar*. It employs a novel heterogeneous disjunctive graph that explicitly models the operation sequences on machines to accurately represent scheduling solutions. Moreover, a memory-enhanced heterogeneous graph neural network (MHGNN) is designed for feature extraction, leveraging historical trajectories to enhance the decision-making capability of the policy network. Finally, a parallel greedy search strategy is adopted to explore the solution space, enabling superior solutions with fewer iterations. Extensive experiments on synthetic data and public benchmarks demonstrate that *MIStar* significantly outperforms both traditional handcrafted improvement heuristics and state-of-the-art DRL-based constructive methods.

1 Introduction

As an emerging paradigm integrating advanced manufacturing and digital technologies, Industry 4.0 is transforming production toward dynamic, large-scale, and customized manufacturing [1, 2]. The job-shop scheduling problem (JSP) [3], a classic NP-hard combinatorial optimization problem (COP), has been widely studied and plays a critical role in manufacturing systems [4]. As an extension of JSP [5, 6], the flexible job-shop scheduling problem (FJSP) allows each operation to be assigned to

*Corresponding author.

39th Conference on Neural Information Processing Systems (NeurIPS 2025).

one of several eligible machines [7], making it more suitable in handling the flexibility and diversity of task–resource relations in new manufacturing paradigms [8]. While this increased flexibility enables FJSP to better meet the demands of mass customization and automation in smart manufacturing (SM) [5, 9, 10], it also introduces greater challenges in developing effective solution strategies [11].

Recent advances in neural models have shown remarkable effectiveness in solving complex COPs [12, 13, 14, 15, 16, 17, 18]. As one promising paradigm among them, Deep Reinforcement Learning (DRL) formulates the scheduling task as a Markov decision process (MDP), learning a parameterized policy network that receives scheduling state as input and outputs feasible actions. DRL approaches to scheduling can be categorized into *construction* and *improvement* [19, 20]. *Construction* methods build schedules by assigning an operation to a machine at each step, progressively extending partial solutions to complete ones [21]. However, their performance heavily relies on state representations [22]. Many studies [23, 24, 25, 26] model scheduling states using disjunctive graphs, but the incompleteness of partial solutions often leads to the omission of important components [21] (e.g., the disjunctive arcs among undispatched operations [23]). Additionally, disjunctive graphs struggle to incorporate essential work-in-progress information required during construction [21] (e.g., current machine load and job status). These limitations lead to suboptimal schedules and reduce their adaptability in SM. In contrast, *improvement* methods start from a complete initial solution and iteratively refine it through small adjustments [27]. As the MDP state represents a fully scheduled solution, it avoids the information loss inherent in partial ones. Moreover, the structure of disjunctive graphs naturally encodes topological relationships among operations [28], enabling complete schedules to be effectively represented with all necessary information [21]. This better supports the high-performance demands of complex scheduling scenarios in SM.

Despite the promising results, most existing DRL-based improvement methods focus only on nonflexible problems, such as the JSP [21, 29]. The increased complexity of FJSP over JSP poses significant challenges for designing effective improvement approaches. First, the one-to-many relationships between operations and machines make the scheduling state more intricate [8], challenging its representation and demanding more expressive neural networks for encoding. Second, improvement methods explore solutions through local moves within neighborhoods. In FJSP, due to the complex decisions involving both operation sequencing and machine assignment [6], this process requires tailored local moves as actions in the MDP [27]. Moreover, the existence of flexibility in FJSP significantly enlarges the solution space, increasing the risk of local optima entrapment and necessitating more efficient search strategies to reduce the extensive number of iterations for convergence [27, 30].

To address the above challenges, we propose a DRL-based improvement heuristic framework for FJSP. First, to represent complex scheduling states, we design a novel heterogeneous disjunctive graph by adding machine nodes with directed hyper-edges to encode the complete solution, effectively capturing critical information about operation sequencing on machines. We also propose a heterogeneous graph neural network and enhance its exploratory capability via a memory module, which stores compact representations of visited solutions and retrieves relevant information to enrich the current state embedding. This module leverages historical schedules to improve decision-making and alleviate local optima issues. Second, we construct the action space based on the Nopt2 neighborhood structure, enabling simultaneous adjustment to operation sequences and machine assignments, and further reduce its dimensionality via constraint relationships to enhance search efficiency. Finally, we propose a parallel greedy exploration strategy that evaluates multiple candidate actions at each step, achieving comparable solution quality with fewer iterations. Extensive experiments on synthetic data and public benchmarks demonstrate the superior performance of our approach in solving FJSP.

The contributions of this paper are summarized as follows: 1) The first DRL-based improvement heuristic framework for FJSP—*MIStar*, capable of learning size-agnostic policies that outperform both traditional handcrafted improvement and state-of-the-art DRL construction methods. 2) An MDP formulation with a heterogeneous disjunctive graph for state representation of complete scheduling solutions in FJSP, and an action space that enables simultaneous adjustments to operation sequences and machine assignments. 3) A memory-enhanced heterogeneous graph neural network (MHGNN) that leverages historical solutions to improve decision-making and alleviate local optima issues. 4) A parallel greedy exploration strategy that improves efficiency of solution space exploration.

2 Related work

This section reviews the limitations of DRL-based construction methods and recent advances in improvement methods, highlighting the challenges in solving FJSP.

Construction methods construct complete solutions by assigning an operation to a machine at each step. Compared to the heuristic guidance offered by conventional dispatching rules, DRL employs DNNs to score actions, but their effectiveness heavily relies on state representations [22, 31, 32]. Early approaches [33, 34, 35, 36] extract multiple general state features as input, which overcompresses state information and neglects the structural nature of FJSP [37]. Recent works [8, 23, 24, 38, 39] integrate GNNs with DRL by modeling scheduling states as graphs, learning rich graph embeddings with structural information for decision-making. However, the incompleteness of partial solutions often results in the omission of important components [21] (e.g., the disjunctive arcs among undispatched operations [23]), and work-in-progress information required during construction is hard to explicitly represent in disjunctive graphs [21], leading to suboptimal performance.

Improvement methods iteratively refine solutions by performing local moves within the neighborhood. Conventional methods use handcrafted rules to greedily select the best solution at each step, but suffer from myopia and costly neighborhood evaluation [21]. Recent studies [21, 29, 40, 41] have addressed these limitations by leveraging deep policy networks in DRL to directly generate local moves. Such DRL-based improvement heuristics were initially applied to routing problems [42, 43, 44] and have since been adapted to scheduling domains. By representing complete solutions as MDP states through disjunctive graphs, these approaches circumvent the inaccuracies in state representation that arise from partial solutions [21]. Falkner et al. [40] train a GNN-based JSP solver using DRL to adapt local search strategies according to problem-specific features. However, their design of local operators relies heavily on expertise, limiting the generalizability. Closer to our work, Zhang et al. [21, 29] represent JSP solutions with disjunctive graphs and define the action space as a set of exchangeable operation pairs based on the N5 neighborhood structure [45], training a GNN-based policy network via DRL. While effective for JSP, extending this framework to FJSP—whose flexible machine assignments better suit mass customization and dynamic production in Industry 4.0 [9, 10]—faces critical challenges. First, conventional disjunctive graphs lack machine nodes, making them insufficient for complex states of FJSP. In addition, the N5-based action design does not account for machine assignment adjustments(See Appendix A for analysis). Furthermore, the increased flexibility of FJSP over JSP enlarges the solution space and aggravates local optima issues in local search [46].

An effective approach to this issue is leveraging memory mechanisms by incorporating past experience to promote exploration [47]. Garmendia et al. [48] maintain a tabu memory to filter redundant visits in routing problems, yet such methods fail to integrate historical data into the decision-making of the policy, leaving historical information underutilized. A closely related work is MARCO [47], which aggregates contextually relevant information from the memory module to enhance state embeddings and improve policy decisions. However, its application in improvement methods is limited to simple binary optimization problems (i.e., maximum cut and maximum independent set), and its approach to information aggregation is unsuitable for the complex constraints in FJSP. In contrast, we simplify scheduling representations, which are stored in the memory module and aggregated via a soft voting mechanism [49] to better accommodate the intricate constraints of FJSP.

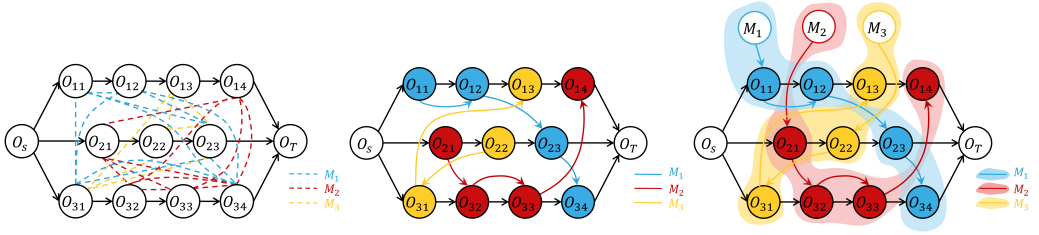

(a) (b) (c)

Figure 1 **Graph representations of FJSP.** (a) FJSP instance in a disjunctive graph; (b) feasible solution in a disjunctive graph; (c) feasible solution in our graph.

3 Preliminaries

This section presents the formulation of FJSP, disjunctive graphs, and Nopt2 neighborhood structure.

Flexible job shop scheduling problem. FJSP is defined as follows: Given a set of jobs $\mathcal{J} = \{J_1, J_2, \cdots, J_n\}$ and a set of machines $\mathcal{M} = \{M_1, M_2, \cdots, M_m\}$, each job J_i consists of n_i operations denoted by $\mathcal{O}_i = \{O_{i_1}, O_{i_2}, \cdots, O_{in_i}\}$. The operations within a job must be processed in a specific order, known as precedence constraints. Each operation O_{ij} can be processed by any machine M_k for a processing time p_{ij}^k from its compatible set $\mathcal{M}_{ij} \subseteq \mathcal{M}$, and the processing is non-preemptive. Each machine can process only one operation at a time. The objective of FJSP is to assign each operation to a compatible machine and determine its processing sequence on the selected machine to minimize the makespan, defined as the maximum completion time $C_{\max} = \max_{i,j}\{C_{ij}\}$, where C_{ij} denotes the completion time of O_{ij}.

Disjunctive graph. An FJSP instance can be represented by a disjunctive graph $G = (\mathcal{O}, \mathcal{C}, \mathcal{D})$ [50]. The operation set $\mathcal{O} = \{O_{ij} \mid \forall i, j\} \cup \{O_S, O_T\}$ includes all operation nodes and two dummy ones representing the start and end states. The conjunctive arc set $\mathcal{C}$ consists of directed arcs that describe the precedence constraints between operations of the same job. The disjunctive arc set $\mathcal{D} = \cup_k \mathcal{D}_k$ comprises undirected edges, and each $\mathcal{D}_k$ connects operations processed on the same machine M_k. In FJSP, each operation can be connected to multiple disjunctive arcs. Therefore, solving an FJSP instance is equivalent to selecting a disjunctive arc for each node and fixing its direction to construct a DAG [28]. In the graph, the longest path from O_S to O_T is called the critical path (CP), whose length represents the makespan of the solution. See Figure 1a and 1b for examples.

The Nopt2 neighbourhood Structure. Given a solution s, the Nopt2 constructs the neighbourhood $Nopt2(s)$ as follows. First, the critical path CP(s) is identified. Then, an operation O_{ij}^k on the critical path is chosen and deleted from its current processing sequence of M_k. It is reinserted into the optimal insertion interval within the sequence of an alternative compatible machine $M_{k'}$ yielding a new solution s'. The optimal insertion interval is determined based on the precedence relations between the newly inserted operation and existing operations on $M_{k'}$, ensuring that all constraints are satisfied and the makespan of s' is potentially reduced. We adopt the Nopt2 neighborhood structure [51] (Figure 2) to define the local move during the search process of *MIStar*. By identifying optimal insertion interval, this structure significantly reduces the size of neighborhood. The neighborhood size $|Nopt2(s)|$ is influenced by both the instance scale and the flexibility of machine selection.

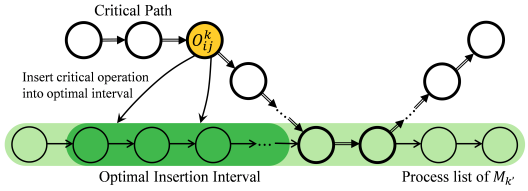

Figure 2 **Nopt2 neighborhood structure.**

4 Methodology

This section details our framework, illustrated in Figure 3. Given an FJSP instance, an initial solution is generated and transformed into a heterogeneous graph, from which a memory-enhanced GNN learns embeddings. The policy network samples several local moves from the neighborhood and evaluates in parallel. The best one is executed to update the current solution, yielding a new one. The process terminates after a predefined search horizon. We formulate the iterative solution optimization as a MDP. This section first formalizes the MDP, then presents a novel heterogeneous graph representation and the memory-enhanced GNN-based policy network. Finally, we describe the parallel greedy exploration strategy and the training algorithm.

4.1 MDP Formulation

We formulate the iterative optimization process of the FJSP as a discrete MDP. At each step t, the agent, the decision-maker based on a given policy, selects an action (local move) from the action space (neighborhood), and the state transitions accordingly to represent a new solution. The MDP is defined as follows.

State. The state s_t encodes a complete solution and is defined by a set of feature vectors, including $\mathbf{x}_{o_{ij}} \in \mathbb{R}^9$ for each operation O_{ij} and $\mathbf{y}_{M_k} \in \mathbb{R}^4$ for each machine M_k, detailed in Appendix B.
Action. The action space $\mathcal{A}_t$ comprises local moves in the Nopt2 neighborhood, changing with

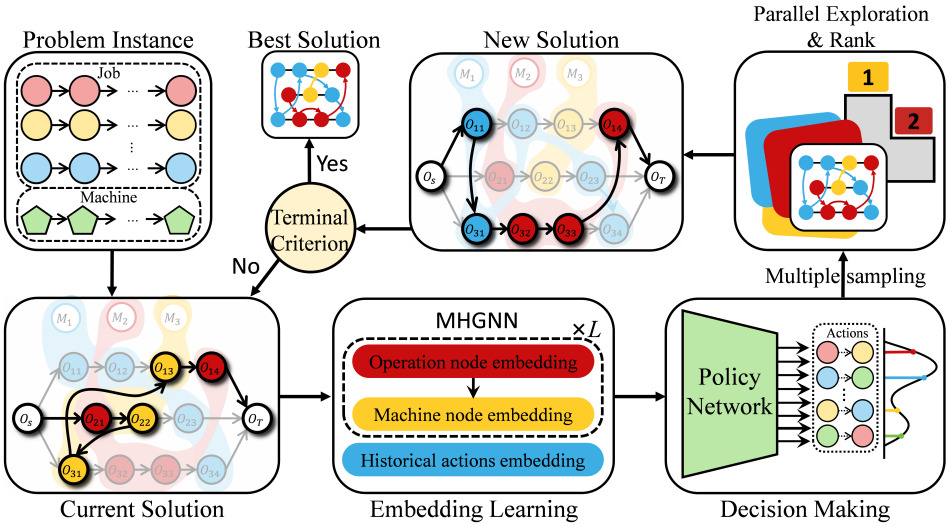

Figure 3 **The architecture of *MIStar*.**

the state s_t. Each action $a_t = [O_m, O_n, M_k]$ denotes inserting critical operation O_m before operation O_n in the processing sequence of machine M_k, where $O_m \notin \{O_S, O_T\}$ and $O_n \neq O_S$. **Reward.** The reward comprises two components: improvement in solution quality r_{gain} and penalty for redundant solution visits $r_{penalty}$. The term r_{gain} measures the improvement over the incumbent best solution s_t^* (initialized as s_0), and is defined as: $r_{gain} = \max(C_{\max}(s_t^*) - C_{\max}(s_{t+1}), 0)$, where maximizing the cumulative reward is equivalent to minimizing the makespan $C_{\max}(s_t^*)$. The term $r_{penalty}$ discourages redundant exploration by evaluating similarity between s_t and previous states. Formally, it is computed as: $r_{penalty} = \lambda \times \frac{1}{K} \sum_{\omega \in \Omega_{\text{TopK}}} \omega$, where Ω_{TopK} denotes the top-K similarity scores between s_t and stored states, and λ is the penalty coefficient. The overall reward is defined as $r_t(s_t, a_t) = r_{gain} - r_{penalty}$, which is initially dominated by makespan improvement and gradually shifts toward solution diversity as improvements diminish.

4.2 Directed Heterogeneous Graph

Conventional disjunctive graphs lack machine nodes, hindering GNNs from accurately capturing machine states in FJSP, which in turn limits policies to effectively maximize machine utilization [37]. Inspired by the heterogeneous disjunctive graph $\mathcal{H}$ [8], we introduce a novel directed heterogeneous disjunctive graph $\overrightarrow{\mathcal{H}} = (\mathcal{O}, \mathcal{M}, \mathcal{C}, \mathcal{E})$ to represent scheduling solutions. In our graph, the operation and machine nodes are denoted as $\mathcal{O}$ and $\mathcal{M}$, while the conjunctive arc set $\mathcal{C}$ and hyper-edge set $\mathcal{E}$ represent the processing sequences on jobs and machines, respectively. Mathematically, the hyper-edge is a special edge that can join any number of vertices [52]. Since machine assignment and processing sequence are fixed in FJSP solutions, we reinterpret $\mathcal{E}$ as a directed hyper-arc set of size $|\mathcal{M}|$, i.e., $\mathcal{E} = \{E^k = (M_k, O^{k1}, O^{k2}, \ldots, O^{kn_k})\}$, where n_k is the number of operations processed on M_k. As shown in Figure 1c, each machine nodes M_k connects to its processing sequence via directed hyper-arcs E^k to explicitly encode machine status, and the unified directed arcs in $\overrightarrow{\mathcal{H}}$ enable clearer delineation and distinction of different solutions. See Appendix C for analysis.

4.3 Memory-enhanced Heterogeneous Graph Neural Network

We propose a memory-enhanced heterogeneous graph neural network (MHGNN) to extract state features from scheduling solutions. As shown in Figure 4, MHGNN encodes the topological and sequential constraint information to generate operation embeddings, which are aggregated into machine nodes to obtain machine embeddings. Meanwhile, relevant historical information is retrieved and extracted as historical action embeddings, which are then concatenated with machine and operation embeddings before being fed into the policy network to produce an action distribution. The following sections detail the embeddings design for operations, machines, and historical information.

4.3.1 Operation Node Embedding

Following [21], we focus on two key aspects of the FJSP graph: (1) the topology dynamically changes due to the transitions of MDP state, and (2) rich semantics are conveyed through two types of neighbors—job predecessors and machine predecessors—reflecting precedence constraints and processing order on machines via conjunctive arcs and hyper-arcs, respectively. Their joint representation is crucial for distinguishing solutions, forming the foundation for scheduling decisions.

To encode the topological information, we employ the Graph Isomorphism Network (GIN) [53], which is known for its strong discriminative power for non-isomorphic graphs. Specifically, given a graph $\overrightarrow{\mathcal{H}} = (\mathcal{O}, \mathcal{M}, \mathcal{C}, \mathcal{E})$, each operation $O_{ij} \in \mathcal{O}$ is encoded into a q-dimensional embedding through an L-layer GIN, where the l-th layer computes as follows:

$$\mu_{O_{ij}}^{l} = \text{MLP}^{l}\left((1+\epsilon^{l}) \cdot \mu_{O_{ij}}^{l-1} + \sum_{U \in N(O_{ij})} \mu_{U}^{l-1}\right) \tag{1}$$

where $\mu_{O_{ij}}^{l} \in \mathbb{R}^{q}$ denotes the topological embedding of operation O_{ij} at layer l, initialized with its raw features $\mathbf{x}_{o_{ij}}$, ϵ^{l} is a learnable parameter, and $N(O_{ij})$ comprises predecessor operation nodes.

To capture rich semantic relationships among operations, we apply an L-layer Graph Attention Network (GAT) with n_H attention heads, with the feature transformation at layer l computed as:

$$\tau_{O_{ij}}^{l} = \text{GAT}^{l}\left(\tau_{O_{ij}}^{l-1}, \{\tau_{U}^{l-1} | U \in N(O_{ij})\}\right) \tag{2}$$

where $\tau_{O_{ij}}^{l} \in \mathbb{R}^{q}$ denotes the semantic embedding of operation O_{ij} at layer l, initialized with raw features $\mathbf{x}_{o_{ij}}$. We obtain the operation embedding $h_{O_{ij}}^{l} \in \mathbb{R}^{2q}$ at layer l by concatenating the above two embeddingshe final-layer outputs form the set of operation node embeddings $\{h_{O_{ij}} = h_{O_{ij}}^{L} \mid \forall O_{ij} \in \mathcal{O}\}$.

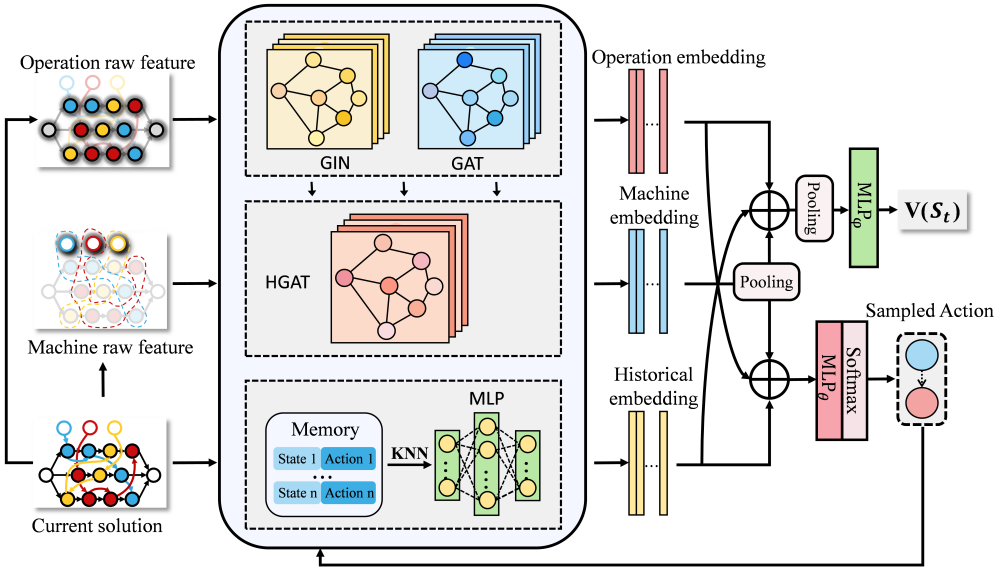

Figure 4 **The network architecture of the memory-enhanced heterogeneou GNN.**

4.3.2 Machine Node Embedding

Machine embeddings are incorporated to capture machine load by aggregating the information of their associated operation nodes, serving as an essential heuristic to guide the policy in reassigning operations from high-load machines to low-load counterparts [8]. For each machine M_k, the hyper-arc $E^{k} = (M_k, O^{k1}, O^{k2}, \ldots, O^{kn_k})$ encodes its full processing sequence. Since the importance of operations at different positions varies, we employ an L-layer heterogeneous GAT [8] to extract machine node embeddings, where nodes with different attributes are processed by distinct linear

transformations rather than a shared one when computing the attention coefficients. The machine node embedding at layer l is computed as follows:

$$h_{M_k}^l = \text{HGAT}^l\left(h_{M_k}^{l-1}, \{h_U^{l-1} | U \in N(M_k)\}\right) \tag{3}$$

where $h_{M_k}^l \in \mathbb{R}^q$ denotes machine embedding at layer l, initialized with raw features $\mathbf{y}_{M_k}$, HGAT^l is a heterogeneous graph attention layer, and $N(M_k)$ comprises operations in its processing sequence. Similarly, the graph-level machine embedding is computed as $h_M = \frac{1}{|\mathcal{M}|}\sum_{M_k \in \mathcal{M}} h_{M_k}^L$.

4.3.3 Historical Action Embedding

At step t, we store the state-action pair (s_t, a_t) in a memory module. To reduce storage and computational costs, we simplify the representation of s_t by omitting node attributes and focusing solely on the processing sequence across machines (see analysis in Appendix D). Specifically, we store the operation-machine incidence matrix $\boldsymbol{L}_t$ at each step, where the non-zero element $(\boldsymbol{L}_t)_{i,j}$ represents the processing order index of operation i on machine j, and assess the similarity between the current state $\boldsymbol{L}_t$ and each historical state $\boldsymbol{L}_{t'}$ ($t' < t$), by computing the Frobenius inner product as their similarity score $\omega_{t,t'} \in \Omega$, given by:

$$\omega_{t,t'} = \langle L_t, L_{t'} \rangle_F = \sum_{i=1}^{|\mathcal{O}|}\sum_{j=1}^{|\mathcal{M}|}(L_t)_{i,j} \cdot (L_{t'})_{i,j} \tag{4}$$

The k-nearest neighbors algorithm retrieves K actions with the highest similarity scores, forming the set $\mathcal{A}_{L_t} = \{a_1, a_2, \ldots, a_K\}$. We aim to aggregate the information in $\mathcal{A}_{L_t}$ to enhance the state embedding and encourage exploration of more diverse solutions through the design of reward. However, each historical action $a_i = [O_{m_i}, O_{n_i}, M_{k_i}]$ is denoted by discrete integer indices indicating operations and machines. Simply weighted averaging yields semantically invalid continuous values, failing to provide useful guidance. To address this, we adopt a soft voting mechanism that aggregates the three dimensions separately based on frequency-weighted similarity, as follows:

$$\tilde{O}_m = \underset{O_m \in \mathcal{A}_{L_t}^1}{\arg\max} \sum_{i=1}^{K} \omega_{t,i} \cdot \mathbb{I}(O_{m_i} = O_m) \tag{5}$$

$$\tilde{O}_n = \underset{O_n \in \mathcal{A}_{L_t}^2}{\arg\max} \sum_{i=1}^{K} \omega_{t,i} \cdot \mathbb{I}(O_{n_i} = O_n) \tag{6}$$

$$\tilde{M}_k = \underset{M_k \in \mathcal{A}_{L_t}^3}{\arg\max} \sum_{i=1}^{K} \omega_{t,i} \cdot \mathbb{I}(M_{k_i} = M_k) \tag{7}$$

where $\omega_{t,i}$ is the similarity score between s_t and the i-th most similar historical state, serving as the weight of a_i, $\mathbb{I}(\cdot)$ is the indicator function, and $\mathcal{A}_{L_t}^1$, $\mathcal{A}_{L_t}^2$ and $\mathcal{A}_{L_t}^3$ denote the unique value sets in each dimension of $\mathcal{A}_{L_t}$. The aggregated action $\tilde{a}_{L_t} = [\tilde{O}_m, \tilde{O}_n, \tilde{M}_k]$ is then mapped by a single-layer MLP to the embedding space of h_O and h_M, resulting in the historical action embedding $h_a \in \mathbb{R}^q$.

4.3.4 Decision Making

Given that machine assignments are determined in FJSP solutions (i.e., for any action $[O_m, O_n, M_k]$, O_n must be processed by M_k), the third dimension can be omitted from the action space. We enhance each operation embedding h_{Oij} by concatenating h_M and h_a, then feed them into the policy network to obtain intermediate vectors forming a matrix $F_O \in \mathbb{R}^{|\mathcal{O}| \times q}$. We multiply F_O by its transpose to obtain a score matrix F_{OO} of shape $|\mathcal{O}| \times |\mathcal{O}|$, where each element represents the priority score of an action in $\mathcal{A}_t$. Based on the Nopt2 neighborhood, we mask infeasible actions by setting their scores to $-\infty$ and apply softmax normalization to obtain the action probability distribution. By leveraging the FJSP constraints, we reduce the space complexity of $\mathcal{A}_t$ from $O(|\mathcal{O}|^2|\mathcal{M}|)$ to $O(|\mathcal{O}|^2)$, which alleviates the difficulty of learning and accelerates model convergence. A detailed analysis of this space complexity reduction is provided in Appendix E.

4.3.5 Training Algorithm

We propose an n-step PPO algorithm with a parallel greedy exploration strategy to efficiently explore the large solution space of FJSP. At each step t, the policy samples P candidate actions

Table 1 Results on small synthetic instances

	Size		Sample		Greedy		100 Iterations				200 Iterations				400 Iterations				OR-Tools[1]
			DANIEL	HGNN	DANIEL	HGNN	GD	FI	BI	MIStar	GD	FI	BI	MIStar	GD	FI	BI	MIStar	
SD1	10×5	Obj.	101.67	105.59	106.76	111.67	**100.00**	100.91	100.55	100.02	100.00	100.91	100.54	**99.88**	100.00	100.91	100.53	**99.69**	
		Gap	5.55%	9.62%	10.84%	15.94%	**3.82%**	4.77%	4.39%	3.84%	3.82%	4.77%	4.38%	**3.70%**	3.82%	4.77%	4.37%	**3.50%**	96.32(5%)
		Time[2]	0.26s	0.44s	0.16s	0.17s	8.13s	12.60s	12.09s	5.64s	16.43s	27.54s	26.21s	11.23s	32.95s	58.71s	54.73s	23.00s	
	20×5	Obj.	192.78	207.53	197.56	211.22	191.31	191.79	191.36	**190.87**	191.31	191.79	191.36	**190.79**	191.31	191.79	191.36	**190.67**	
		Gap	2.46%	10.30%	5.00%	12.26%	1.68%	1.93%	1.71%	**1.45%**	1.68%	1.93%	1.71%	**1.40%**	1.68%	1.93%	1.71%	**1.34%**	188.15(0%)
		Time	1.14s	1.05s	0.33s	0.34s	53.86s	70.73s	77.32s	15.72s	1.80m	2.46m	2.70m	33.38s	3.60m	5.20m	5.56m	1.16m	
	15×10	Obj.	153.22	160.86	161.28	166.92	151.96	152.10	151.90	**150.85**	151.96	152.10	151.90	**150.61**	151.96	152.10	151.90	**150.34**	
		Gap	6.75%	12.07%	12.37%	16.30%	5.87%	5.97%	5.83%	**5.10%**	5.87%	5.97%	5.83%	**4.93%**	5.87%	5.97%	5.83%	**4.74%**	143.53(7%)
		Time	1.90s	2.17s	0.50s	0.50s	58.62s	86.43s	90.21s	27.09s	1.97m	3.08m	3.11m	54.22s	3.93m	6.81m	6.33m	1.80m	
	20×10	Obj.	193.91	214.81	198.50	215.78	192.92	193.26	193.03	**192.71**	192.92	193.26	193.03	**192.70**	192.92	193.26	193.03	**192.68**	
		Gap	-1.06%	9.61%	1.29%	10.10%	-1.56%	-1.39%	-1.51%	**-1.67%**	-1.56%	-1.39%	-1.51%	**-1.67%**	-1.56%	-1.39%	-1.51%	**-1.68%**	195.98(0%)
		Time	2.71s	2.93s	0.68s	0.69s	2.44m	2.90m	3.09m	32.91s	4.90m	6.06m	6.64m	1.14m	9.86m	12.83m	13.87m	2.51m	
SD2	10×5	Obj.	365.26	479.37	413.73	552.80	360.17	354.22	349.66	**345.05**	360.17	354.22	349.66	**343.43**	360.17	354.22	349.66	**342.50**	
		Gap	11.96%	46.94%	26.82%	69.45%	10.40%	8.58%	7.18%	**5.77%**	10.40%	8.58%	7.18%	**5.27%**	10.40%	8.58%	7.18%	**4.98%**	326.24(96%)
		Time	0.30s	0.22s	0.16s	0.20s	6.06s	10.37s	11.74s	5.27s	12.21s	22.48s	25.65s	10.33s	24.39s	48.51s	54.57s	21.39s	
	20×5	Obj.	629.56	960.11	671.38	1047.83	626.35	622.75	619.13	**615.12**	626.35	622.75	619.13	**613.75**	626.35	622.75	619.13	**612.73**	
		Gap	4.57%	59.48%	11.52%	74.05%	4.04%	3.44%	2.84%	**2.17%**	4.04%	3.44%	2.84%	**1.95%**	4.04%	3.44%	2.84%	**1.78%**	602.04(0%)
		Time	0.78s	0.77s	0.33s	0.35s	48.48s	62.37s	72.23s	11.55s	1.61m	2.18m	2.52m	23.50s	3.30m	4.71m	5.21m	47.93s	
	15×10	Obj.	522.51	757.18	588.72	824.62	516.79	511.00	514.73	**488.22**	516.79	511.00	514.73	**476.93**	516.79	511.00	514.73	**465.71**	
		Gap	38.53%	100.75%	56.09%	118.63%	37.02%	35.48%	36.47%	**29.44%**	37.02%	35.48%	36.47%	**26.45%**	37.02%	35.48%	36.47%	**23.47%**	377.17(28%)
		Time	1.72s	1.45s	0.50s	0.57s	60.34s	89.27s	78.09s	18.09s	2.07m	3.17m	2.64m	37.42s	4.19m	6.87m	5.30m	1.31m	
	20×10	Obj.	552.38	987.57	605.37	1036.65	549.30	542.39	535.06	**530.93**	549.30	542.39	535.06	**528.92**	549.30	542.39	535.06	**525.49**	
		Gap	19.01%	112.76%	30.42%	123.34%	18.34%	16.85%	15.27%	**14.39%**	18.34%	16.85%	15.27%	**13.95%**	18.34%	16.85%	15.27%	**13.21%**	464.16(1%)
		Time	2.84s	2.91s	0.69s	0.71s	2.35m	3.06m	3.53m	25.76s	4.64m	7.07m	7.54m	53.25s	9.14m	15.33m	15.76m	1.88m	

[1] For OR-Tools, the solution and the ratio of optimally solved instances are reported.
[2] "s", "m", and "h" denote seconds, minutes, and hours, respectively.

$\{a_t^1, a_t^2, \ldots, a_t^P\}$ from A_t, evaluates their improvements in parallel, and selects the action a_t^i yielding the greatest makespan reduction for execution. This approach enables the exploration of P solutions per iteration, producing high-quality solutions in fewer iterations and significantly reducing search time. More detailed analysis and pseudo-code of our training algorithm are presented in Appendix F.

5 Experiments

In this section, we present the experimental setup, performance evaluations on synthetic and public datasets as well as the results of ablation studies.

5.1 Experimental Settings

Datasets. We evaluate our method on both synthetic data and benchmarks. The synthetic datasets SD1 [8] and SD2 [22] cover 6 scales and 100 instances per scale, and differ in distribution. For each $n \times m$ FJSP instance, the number of compatible machines $|\mathcal{M}_{ij}|$ for O_{ij} is sampled from $U(1, m)$. In SD1, the number of operations per job and the average processing time $\overline{p}_{ij}$ of O_{ij} are sampled from $U(0.8 \times m, 1.2 \times m)$ and $U(1, 20)$, respectively. The machine-specific processing time p_{ij}^k is drawn from $U(0.8 \times \overline{p}_{ij}, 1.2 \times \overline{p}_{ij})$. While in SD2, each job has m operations, and p_{ij}^k is sampled from $U(1, 99)$. Benchmarks include Hurink [54] (Edata, Rdata, Vdata; 40 instances per set over 8 scales) and Brandimarte [55] (10 instances across 7 scales). Implementation details are in Appendix G.

Baselines and Performance Metrics. We compare our method with two DRL-based construction methods, HGNN [8] and DANIEL [22]. HGNN is a heterogeneous GNN designed to encode features represented by a heterogeneous disjunctive graph, while DANIEL employs a dual-attention network on tight graph representation. Both models are retrained and tested, with results reported for sampling and greedy strategies. We also compare three hand-crafted improvement rules: greedy(GD) [46], best-improvement (BI), and first-improvement (FI) [56]. Specifically, GD selects the solution with the smallest makespan from the neighborhood, while BI and FI choose the best and first improving ones, respectively. A *restart* strategy [57] is applied in BI and FI to escape local optima by continuing the search from a new initial solution. We also compares with (near-)optimal solutions from Google OR-Tools, a powerful constraint programming solver, under a 1800 s time limit. For benchmarks, we report the results of a two-stage genetic algorithm (2SGA) [58] directly from [22].

As such incremental search methods cannot quickly access very different solutions [27, 42], their performance is sensitive to the initial solution quality. We use DANIEL to sample 100 initial solutions per instance, which are equally applied to three rule-based methods for fair comparison. *MIStar* then performs parallel iterative search, retaining the best solution. Performance is measured by the average makespan and the relative gap to the best-known solution, which is obtained via OR-Tools for synthetic datasets [22] and from [59] for public benchmarks.

Table 2 Generalization results on large synthetic instances

	Size	Sample		Greedy		100 Iterations				200 Iterations				400 Iterations				OR-Tools[1]
		DANIEL	HGNN	DANIEL	HGNN	GD	FI	BI	MIStar	GD	FI	BI	MIStar	GD	FI	BI	MIStar	
SD1	Obj.	286.77	308.55	288.61	314.71	286.04	286.19	285.95	**285.79**	286.04	286.19	285.95	**285.75**	286.04	286.19	285.95	**285.68**	
	30×10 Gap	4.41%	12.33%	5.08%	14.58%	4.14%	4.19%	4.11%	**4.05%**	4.14%	4.19%	4.11%	**4.03%**	4.14%	4.19%	4.11%	**4.01%**	274.67(6%)
	Time[2]	5.60s	6.25s	0.97s	0.97s	7.67m	10.51m	10.73m	57.03s	15.32m	22.00m	21.49m	1.83m	30.65m	47.10m	43.11m	3.77m	
	Obj.	379.71	410.76	379.28	417.87	379.04	379.05	378.92	**378.82**	379.04	379.05	378.92	**378.76**	379.04	379.05	378.92	**378.63**	
	40×10 Gap	3.76%	12.24%	3.64%	14.18%	3.57%	3.58%	3.54%	**3.51%**	3.57%	3.58%	3.54%	**3.50%**	3.57%	3.58%	3.54%	**3.46%**	365.96(3%)
	Time	9.94s	10.45s	1.30s	1.34s	18.20m	25.13m	24.04m	1.11m	36.48m	52.01m	48.46m	2.55m	1.22h	1.82h	1.63h	5.94m	
SD2	Obj.	756.52	1453.40	800.02	1536.74	753.66	748.41	739.47	**735.14**	753.66	748.41	739.47	**731.84**	753.66	748.41	739.47	**728.76**	
	30×10 Gap	9.28%	109.95%	15.57%	121.99%	8.87%	8.11%	6.82%	**6.19%**	8.87%	8.11%	6.82%	**5.72%**	8.87%	8.11%	6.82%	**5.27%**	692.26(0%)
	Time	5.76s	5.98s	0.99s	1.14s	7.65m	12.13m	12.16m	49.43s	15.04m	24.58m	25.49m	1.69m	29.50m	51.78m	52.62m	3.56m	
	Obj.	953.14	1937.96	984.55	2045.78	947.64	941.60	**930.44**	931.04	947.64	941.60	930.44	**929.13**	947.64	941.60	930.44	**925.93**	
	40×10 Gap	-4.53%	94.11%	-1.39%	104.91%	-5.08%	-5.69%	**-6.81%**	-6.75%	-5.08%	-5.69%	-6.81%	**-6.94%**	-5.08%	-5.69%	-6.81%	**-7.26%**	998.39(0%)
	Time	10.06s	11.10s	1.34s	1.36s	18.29m	25.07m	21.06m	73.29s	35.83m	54.84m	42.18m	2.52m	1.18h	1.89h	1.42h	5.40m	

[1] For OR-Tools, the solution and the ratio of optimally solved instances are reported.
[2] "s", "m", and "h" denote seconds, minutes, and hours, respectively.

Table 3 Results on public benchmarks

Method	mk			la(rdata)			la(edata)			la(vdata)		
	Obj.	Gap	Time(s)	Obj.	Gap	Time(s)	Obj.	Gap	Time(s)	Obj.	Gap	Time(s)
OR-Tools	174.20	0.99%	1447.08	935.80	0.16%	1397.43	1028.93	0.01%	899.60	919.60	-0.01%	639.17
2SGA	175.20	1.57%	57.60		-			-		812.20[1]	0.39%	51.43
DANIEL(S)[2]	180.80	4.81%	1.71	984.63	5.39%	1.99	1120.28	8.88%	2.00	934.75	1.64%	2.02
HGNN(S)	192.20	11.42%	1.72	1004.60	7.53%	1.84	1123.10	9.16%	2.44	934.23	1.58%	2.12
DANIEL(G)	184.30	6.84%	0.45	1044.85	11.84%	0.48	1176.40	14.34%	0.48	965.38	4.97%	0.48
HGNN(G)	200.00	15.94%	0.46	1035.75	10.86%	0.52	1189.33	15.59%	0.48	962.48	4.66%	0.47
GD-100[3]	178.92	3.72%	22.86	963.03	3.08%	26.09	1100.46	6.96%	4.14	924.53	0.53%	89.94
FI-100	178.85	3.68%	34.91	968.60	3.67%	36.16	1101.43	7.05%	6.77	927.33	0.83%	131.90
BI-100	178.43	3.44%	37.98	964.80	3.27%	41.25	1100.63	6.97%	5.91	927.55	0.86%	122.02
MIStar-100	**177.80** (±0.74)[4]	**3.07%**	17.50	**958.90** (±4.55)	**2.64%**	19.86	**1099.38** (±4.17)	**6.85%**	19.60	**923.55** (±1.81)	**0.42%**	20.36
GD-200	178.92	3.72%	45.73	963.03	3.08%	51.94	1100.46	6.96%	8.27	924.53	0.53%	179.99
FI-200	178.85	3.68%	74.64	968.60	3.67%	76.17	1101.43	7.05%	14.45	927.33	0.83%	272.34
BI-200	178.43	3.44%	81.03	964.65	3.25%	86.20	1100.60	6.97%	12.70	926.55	0.75%	251.11
MIStar-200	**177.70** (±0.75)	**3.01%**	36.45	**957.23** (±4.72)	**2.46%**	40.66	**1099.30** (±4.13)	**6.84%**	40.05	**922.70** (±1.71)	**0.33%**	41.83
GD-400	178.92	3.72%	91.79	963.03	3.08%	103.81	1100.46	6.96%	16.51	924.53	0.53%	360.28
FI-400	178.85	3.68%	162.16	968.60	3.67%	158.27	1101.35	7.04%	31.56	927.33	0.83%	586.32
BI-400	178.43	3.44%	169.70	964.50	3.24%	180.45	1100.33	6.94%	27.24	925.55	0.64%	521.21
MIStar-400	**177.60** (±0.63)	**2.96%**	76.35	**956.38** (±4.04)	**2.37%**	85.45	**1099.18** (±4.25)	**6.83%**	83.77	**921.85** (±1.77)	**0.24%**	87.23

[1] The makespan and gap of 2SGA on la(vdata) benchmark are computed on la1-30 instances, as reported in [58].
[2] "(S)" denotes the sampling strategy, and "(G)" denotes the greedy strategy.
[3] "-100", "-200", and "-400" denote different iteration budgets.
[4] Values are reported as the average (± standard deviation) over 10 independent runs.

5.2 Performance on Synthetic Instances

We train our model with 100 iterations on four small sizes (10×5, 20×5, 15×10, and 20×10) from two synthetic datasets and evaluate on corresponding test instances. Table 1 reports the performance and average runtime per instance across all methods. The generalization capability of the model, evaluated on large-sized instances (30×10 and 40×10 in Table 2) and with extended iterations up to 400, is also reported. The results show that *MIStar* consistently outperforms two construction methods across various instances, with larger gains on SD2. This is because initial solutions on SD1 are near-optimal, leaving limited room for improvement, as verified by experiments on varying-quality initial solutions (see Appendix I). Compared with rule-based improvement heuristics, *MIStar* achieves better solution quality with shorter runtime and maintains consistent improvement over longer iterations, verifying the effectiveness and efficiency of its policy. See detailed analysis in Appendix H.

5.3 Performance on Public Benchmarks

We evaluate generalization on Hurink and Brandimarte benchmarks using the model trained on the 10×5 instances from SD2. While OR-Tools and 2SGA achieve near-optimal results, their computational cost limits practicality. *MIStar* maintains stable performance over both DRL-based construction and rule-base method across all benchmarks, demonstrating its effective generalization through the learned general policy. Regarding solving time, rule-based methods exhibit notable variation across Hurink dataset, with runtimes increasing from `edata` to `rdata` and `vdata` due to the growing set of assignable machines that enlarge the neighborhood. In contrast, *MIStar* maintains stable runtime across all distributions.

Table 4 Generalization Performance on Larger-Scale Instances

Instance Size	Method	Objective	Time (min)	Optimality Gap
50×15	OR-Tools	881.45	60.0	39.05%
(LB:537.2)	MIStar-200	969.7	10.6	44.60%
60×15	OR-Tools	1075.1	60.0	46.94%
(LB:570.2)	MIStar-200	1109.8	14.2	48.62%
100×10	OR-Tools	1922.65	60.0	62.22%
(LB:726.5)	MIStar-200	2138.4	15.9	66.03%
50×30	OR-Tools	Infeasible	60.0	-
(LB:N/A)	MIStar-200	1040.1	60.0	-

5.4 Results on Larger Instances

To further evaluate the generalization and scalability of our framework, we conducted experiments on even larger instances (up to 1,500 operations). For each problem size, 10 instances were randomly generated, and both *MIStar* and OR-Tools were given a one-hour time limit per instance. We report their average optimality gap across different scales, whcih is calculated based on the Lower Bound (LB) as $\left(1 - \frac{\text{LB}}{\text{Objective}}\right) \times 100\%$. For *MIStar*, the results were measured at 200 iterations using the model trained on instances of size 20×15.

The results in Table 4 highlight two critical advantages of our approach. First and most strikingly, on the highly complex 50×30 instances, OR-Tools failed to produce any feasible solution within the time limit, whereas *MIStar* consistently found high-quality solutions. This demonstrates *MIStar*'s superior robustness and scalability on truly challenging problems. Second, for the other large instances where OR-Tools did find a solution, *MIStar* achieves comparable solution quality in a small fraction of the time. For example, on the 100×10 instances, *MIStar* reaches a 66.03% optimality gap in just under 16 minutes, while OR-Tools requires a full hour to achieve a 62.22% gap. This massive speed-up, combined with the strong generalization from a model trained only on smaller instances, confirms that *MIStar* provides an effective and highly scalable solution for large-scale FJSP.

5.5 Ablation Studies

We conducted ablation experiments on the SD2 dataset to assess the memory module and parallel greedy search strategy. As evidenced in Table 7 (Appendix J), their combination improves performance: the parallel greedy search strategy significantly enhances search efficiency and mitigates the risk of early convergence to local optima. Meanwhile, the memory module optimizes policy decisions, leading to higher solution quality. We further investigated the impact of the parallel scale P on our strategy. Figure 8 (Appendix J) demonstrates that increasing P generally improves performance at the cost of longer runtimes, with the optimal value depending on the instance characteristics. Therefore, P should be properly adjusted to achieve a trade-off between runtime and solution quality.

6 Conclusion

This study proposes *MIStar*, the first DRL-based improvement heuristic framework for solving the FJSP. By formulating the iterative refinement as an MDP, we introduce a heterogeneous disjunctive graph representation tailored for FJSP solutions and employ a memory-enhanced heterogeneous graph neural network for feature extraction and thorough exploration of the solution space. Furthermore, we propose a parallel greedy search strategy that significantly reduces the number of iterations while achieving high-quality solutions. Extensive experiments on synthetic data and public benchmarks demonstrate the superior performance of *MIStar* over both traditional handcrafted improvement heuristics and DRL-based construction methods. Future work may focus on enabling the network to adaptively adjust the parallel scale P, and on extending our methodology to disruptive local moves in larger neighborhoods, such as the reconstruction of solution segments, to further enhance exploration and reduce sensitivity to initial solutions.

Acknowledgements

This work is supported by the Jilin Provincial Department of Science and Technology Project under Grant Grant20240101369JC.

References

[1] Heiner Lasi, Peter Fettke, Hans-Georg Kemper, Thomas Feld, and Michael Hoffmann. Industry 4.0. *Business & information systems engineering*, 6:239–242, 2014.

[2] Yi Wang, Hai-Shu Ma, Jing-Hui Yang, and Ke-Sheng Wang. Industry 4.0: a way from mass customization to mass personalization production. *Advances in manufacturing*, 5(4):311–320, 2017.

[3] Runwei Cheng, Mitsuo Gen, and Yasuhiro Tsujimura. A tutorial survey of job-shop scheduling problems using genetic algorithms—i. representation. *Computers & industrial engineering*, 30(4):983–997, 1996.

[4] Jian Zhang, Guofu Ding, Yisheng Zou, Shengfeng Qin, and Jianlin Fu. Review of job shop scheduling research and its new perspectives under industry 4.0. *Journal of intelligent manufacturing*, 30:1809–1830, 2019.

[5] Jin Xie, Liang Gao, Kunkun Peng, Xinyu Li, and Haoran Li. Review on flexible job shop scheduling. *IET collaborative intelligent manufacturing*, 1(3):67–77, 2019.

[6] Imran Ali Chaudhry and Abid Ali Khan. A research survey: review of flexible job shop scheduling techniques. *International Transactions in Operational Research*, 23(3):551–591, 2016.

[7] Guohui Zhang, Xinyu Shao, Peigen Li, and Liang Gao. An effective hybrid particle swarm optimization algorithm for multi-objective flexible job-shop scheduling problem. *Computers & Industrial Engineering*, 56(4):1309–1318, 2009.

[8] Wen Song, Xinyang Chen, Qiqiang Li, and Zhiguang Cao. Flexible job-shop scheduling via graph neural network and deep reinforcement learning. *IEEE Transactions on Industrial Informatics*, 19(2):1600–1610, 2022.

[9] Pedro Coelho, Ana Pinto, Samuel Moniz, and Cristovão Silva. Thirty years of flexible job-shop scheduling: a bibliometric study. *Procedia Computer Science*, 180:787–796, 2021.

[10] Philipp Wenzelburger and Frank Allgöwer. Model predictive control for flexible job shop scheduling in industry 4.0. *Applied Sciences*, 11(17):8145, 2021.

[11] Stéphane Dauzère-Pérès, Junwen Ding, Liji Shen, and Karim Tamssaouet. The flexible job shop scheduling problem: A review. *European Journal of Operational Research*, 314(2):409–432, 2024.

[12] Yoshua Bengio, Andrea Lodi, and Antoine Prouvost. Machine learning for combinatorial optimization: a methodological tour d'horizon. *European Journal of Operational Research*, 290(2):405–421, 2021.

[13] Mingzhao Wang, You Zhou, Zhiguang Cao, Yubin Xiao, Xuan Wu, Wei Pang, Yuan Jiang, Hui Yang, Peng Zhao, and Yuanshu Li. An efficient diffusion-based non-autoregressive solver for traveling salesman problem. In *Proceedings of the 31st ACM SIGKDD Conference on Knowledge Discovery and Data Mining V.1*, page 1469–1480, 2025.

[14] Yubin Xiao, Di Wang, Boyang Li, Mingzhao Wang, Xuan Wu, Changliang Zhou, and You Zhou. Distilling autoregressive models to obtain high-performance non-autoregressive solvers for vehicle routing problems with faster inference speed. In *Proceedings of the AAAI Conference on Artificial Intelligence*, volume 38, pages 20274–20283, 2024.

[15] Yubin Xiao, Di Wang, Boyang Li, Huanhuan Chen, Wei Pang, Xuan Wu, Hao Li, Dong Xu, Yanchun Liang, and You Zhou. Reinforcement learning-based nonautoregressive solver for traveling salesman problems. *IEEE Transactions on Neural Networks and Learning Systems*, pages 1–15, 2024.

[16] Yubin Xiao, Di Wang, Xuan Wu, Yuesong Wu, Boyang Li, Wei Du, Liupu Wang, and You Zhou. Improving generalization of neural vehicle routing problem solvers through the lens of model architecture. *Neural Networks*, 187:107380, 2025.

[17] Yubin Xiao, Yuesong Wu, Rui Cao, Di Wang, Zhiguang Cao, Peng Zhao, and Yuan Jiang. Dgl: Dynamic global-local information aggregation for scalable vrp generalization with self-improvement learning. In *Proceedings of the International Joint Conference on Artificial Intelligence (IJCAI)*, 2025.

[18] Xuan Wu, Di Wang, Chunguo Wu, Lijie Wen, Chunyan Miao, Yubin Xiao, and You Zhou. Efficient heuristics generation for solving combinatorial optimization problems using large language models. In *Proceedings of the 31st ACM SIGKDD Conference on Knowledge Discovery and Data Mining V. 2*, pages 3228–3239, 2025.

[19] Xuan Wu, Di Wang, Lijie Wen, Yubin Xiao, Chunguo Wu, Yuesong Wu, Chaoyu Yu, Douglas L. Maskell, and You Zhou. Neural combinatorial optimization algorithms for solving vehicle routing problems: A comprehensive survey with perspectives, 2024.

[20] Nina Mazyavkina, Sergey Sviridov, Sergei Ivanov, and Evgeny Burnaev. Reinforcement learning for combinatorial optimization: A survey. *Computers & Operations Research*, 134:105400, 2021.

[21] Cong Zhang, Zhiguang Cao, Wen Song, Yaoxin Wu, and Jie Zhang. Deep reinforcement learning guided improvement heuristic for job shop scheduling. In *The Twelfth International Conference on Learning Representations*, 2024.

[22] Runqing Wang, Gang Wang, Jian Sun, Fang Deng, and Jie Chen. Flexible job shop scheduling via dual attention network-based reinforcement learning. *IEEE Transactions on Neural Networks and Learning Systems*, 35(3):3091–3102, 2023.

[23] Cong Zhang, Wen Song, Zhiguang Cao, Jie Zhang, Puay Siew Tan, and Xu Chi. Learning to dispatch for job shop scheduling via deep reinforcement learning. *Advances in neural information processing systems*, 33:1621–1632, 2020.

[24] Kun Lei, Peng Guo, Wenchao Zhao, Yi Wang, Linmao Qian, Xiangyin Meng, and Liansheng Tang. A multi-action deep reinforcement learning framework for flexible job-shop scheduling problem. *Expert Systems with Applications*, 205:117796, 2022.

[25] Ruiqi Chen, Wenxin Li, and Hongbing Yang. A deep reinforcement learning framework based on an attention mechanism and disjunctive graph embedding for the job-shop scheduling problem. *IEEE Transactions on Industrial Informatics*, 19(2):1322–1331, 2022.

[26] Junyoung Park, Jaehyeong Chun, Sang Hun Kim, Youngkook Kim, and Jinkyoo Park. Learning to schedule job-shop problems: representation and policy learning using graph neural network and reinforcement learning. *International journal of production research*, 59(11):3360–3377, 2021.

[27] Nathan Grinsztajn, Daniel Furelos-Blanco, Shikha Surana, Clément Bonnet, and Tom Barrett. Winner takes it all: Training performant rl populations for combinatorial optimization. *Advances in Neural Information Processing Systems*, 36:48485–48509, 2023.

[28] Egon Balas. Machine sequencing via disjunctive graphs: an implicit enumeration algorithm. *Operations research*, 17(6):941–957, 1969.

[29] Cong Zhang, Zhiguang Cao, Yaoxin Wu, Wen Song, and Jing Sun. Learning topological representations with bidirectional graph attention network for solving job shop scheduling problem. In *Proceedings of the Fortieth Conference on Uncertainty in Artificial Intelligence*, 2024.

[30] Ke Li, Fei Liu, Zhenkun Wang, and Qingfu Zhang. Destroy and repair using hyper-graphs for routing. In *Proceedings of the AAAI Conference on Artificial Intelligence*, volume 39, pages 18341–18349, 2025.

[31] Peng Zhao, You Zhou, Di Wang, Zhiguang Cao, Yubin Xiao, Xuan Wu, Yuanshu Li, Hongjia Liu, Wei Du, Yuan Jiang, and Liupu Wang. Dual operation aggregation graph neural networks for solving flexible job-shop scheduling problem with reinforcement learning. In *Proceedings of the ACM Web Conference 2025*, 2025.

[32] Peng Zhao, Zhiguang Cao, Di Wang, Wen Song, Wei Pang, You Zhou, and Yuan Jiang. Visual-enhanced multimodal framework for flexible job shop scheduling problem. In *Proceedings of the 33rd ACM International Conference on Multimedia*, 2025.

[33] Shu Luo. Dynamic scheduling for flexible job shop with new job insertions by deep reinforcement learning. *Applied Soft Computing*, 91:106208, 2020.

[34] Yi Feng, Lu Zhang, Zhile Yang, Yuanjun Guo, and Dongsheng Yang. Flexible job shop scheduling based on deep reinforcement learning. In *2021 5th Asian Conference on Artificial Intelligence Technology (ACAIT)*, pages 660–666. IEEE, 2021.

[35] Shu Luo, Linxuan Zhang, and Yushun Fan. Dynamic multi-objective scheduling for flexible job shop by deep reinforcement learning. *Computers & Industrial Engineering*, 159:107489, 2021.

[36] Renke Liu, Rajesh Piplani, and Carlos Toro. Deep reinforcement learning for dynamic scheduling of a flexible job shop. *International Journal of Production Research*, 60(13):4049–4069, 2022.

[37] Lanjun Wan, Long Fu, Changyun Li, and Keqin Li. Flexible job shop scheduling via deep reinforcement learning with meta-path-based heterogeneous graph neural network. *Knowledge-Based Systems*, 296:111940, 2024.

[38] Zhengqi Zeng, Xiaoxia Li, and Changbo Bai. A deep reinforcement learning approach to flexible job shop scheduling. In *2022 IEEE International Conference on Systems, Man, and Cybernetics (SMC)*, pages 884–890. IEEE, 2022.

[39] Wenquan Zhang, Fei Zhao, Yong Li, Chao Du, Xiaobing Feng, and Xuesong Mei. A novel collaborative agent reinforcement learning framework based on an attention mechanism and disjunctive graph embedding for flexible job shop scheduling problem. *Journal of Manufacturing Systems*, 74:329–345, 2024.

[40] Jonas K Falkner, Daniela Thyssens, Ahmad Bdeir, and Lars Schmidt-Thieme. Learning to control local search for combinatorial optimization. In *Joint European Conference on Machine Learning and Knowledge Discovery in Databases*, pages 361–376. Springer, 2022.

[41] Constantin Waubert de Puiseau, Fabian Wolz, Merlin Montag, Jannik Peters, Hasan Tercan, and Tobias Meisen. Decision transformer for enhancing neural local search on the job shop scheduling problem. *arXiv e-prints*, pages arXiv–2409, 2024.

[42] Xinyun Chen and Yuandong Tian. Learning to perform local rewriting for combinatorial optimization. *Advances in neural information processing systems*, 32, 2019.

[43] Hao Lu, Xingwen Zhang, and Shuang Yang. A learning-based iterative method for solving vehicle routing problems. In *International conference on learning representations*, 2019.

[44] Yaoxin Wu, Wen Song, Zhiguang Cao, Jie Zhang, and Andrew Lim. Learning improvement heuristics for solving routing problems. *IEEE transactions on neural networks and learning systems*, 33(9):5057–5069, 2021.

[45] ChaoYong Zhang, PeiGen Li, ZaiLin Guan, and YunQing Rao. A tabu search algorithm with a new neighborhood structure for the job shop scheduling problem. *Computers & Operations Research*, 34(11):3229–3242, 2007.

[46] Eugeniusz Nowicki and Czeslaw Smutnicki. A fast taboo search algorithm for the job shop problem. *Management science*, 42(6):797–813, 1996.

[47] Andoni I Garmendia, Quentin Cappart, Josu Ceberio, and Alexander Mendiburu. Marco: A memory-augmented reinforcement framework for combinatorial optimization. *arXiv preprint arXiv:2408.02207*, 2024.

[48] Andoni I Garmendia, Josu Ceberio, and Alexander Mendiburu. Neural improvement heuristics for graph combinatorial optimization problems. *IEEE Transactions on Neural Networks and Learning Systems*, 2023.

[49] Zhi-Hua Zhou. *Ensemble methods: foundations and algorithms*. CRC press, 2025.

[50] Igor G Smit, Jianan Zhou, Robbert Reijnen, Yaoxin Wu, Jian Chen, Cong Zhang, Zaharah Bukhsh, Yingqian Zhang, and Wim Nuijten. Graph neural networks for job shop scheduling problems: A survey. *Computers & Operations Research*, page 106914, 2024.

[51] Monaldo Mastrolilli and Luca Maria Gambardella. Effective neighbourhood functions for the flexible job shop problem. *Journal of scheduling*, 3(1):3–20, 2000.

[52] Alain Bretto. Hypergraph theory. *An introduction. Mathematical Engineering. Cham: Springer*, 1:209–216, 2013.

[53] Keyulu Xu, Weihua Hu, Jure Leskovec, and Stefanie Jegelka. How powerful are graph neural networks? *arXiv preprint arXiv:1810.00826*, 2018.

[54] Johann Hurink, Bernd Jurisch, and Monika Thole. Tabu search for the job-shop scheduling problem with multi-purpose machines. *Operations-Research-Spektrum*, 15:205–215, 1994.

[55] Paolo Brandimarte. Routing and scheduling in a flexible job shop by tabu search. *Annals of Operations research*, 41(3):157–183, 1993.

[56] Pierre Hansen and Nenad Mladenović. First vs. best improvement: An empirical study. *Discrete Applied Mathematics*, 154(5):802–817, 2006.

[57] Helena Ramalhinho Lourenço, Olivier C Martin, and Thomas Stützle. Iterated local search: Framework and applications. In *Handbook of metaheuristics*, pages 129–168. Springer, 2018.

[58] Danial Rooyani and Fantahun M Defersha. An efficient two-stage genetic algorithm for flexible job-shop scheduling. *Ifac-Papersonline*, 52(13):2519–2524, 2019.

[59] Dennis Behnke and Martin Josef Geiger. Test instances for the flexible job shop scheduling problem with work centers. 2012.

[60] Anssi Kanervisto, Christian Scheller, and Ville Hautamäki. Action space shaping in deep reinforcement learning. In *2020 IEEE conference on games (CoG)*, pages 479–486. IEEE, 2020.

[61] John Schulman, Filip Wolski, Prafulla Dhariwal, Alec Radford, and Oleg Klimov. Proximal policy optimization algorithms. *arXiv preprint arXiv:1707.06347*, 2017.

NeurIPS Paper Checklist

1. **Claims**

   Question: Do the main claims made in the abstract and introduction accurately reflect the paper's contributions and scope?

   Answer: [Yes]

   Justification: Please see abstract and Section 1, which accurately reflect the paper's contributions and scope.

   Guidelines:

   - The answer NA means that the abstract and introduction do not include the claims made in the paper.
   - The abstract and/or introduction should clearly state the claims made, including the contributions made in the paper and important assumptions and limitations. A No or NA answer to this question will not be perceived well by the reviewers.
   - The claims made should match theoretical and experimental results, and reflect how much the results can be expected to generalize to other settings.
   - It is fine to include aspirational goals as motivation as long as it is clear that these goals are not attained by the paper.

2. **Limitations**

   Question: Does the paper discuss the limitations of the work performed by the authors?

   Answer: [Yes]

   Justification: The limitations of this work are discussed in Section 5.1 and Section 6.

   Guidelines:

   - The answer NA means that the paper has no limitation while the answer No means that the paper has limitations, but those are not discussed in the paper.
   - The authors are encouraged to create a separate "Limitations" section in their paper.
   - The paper should point out any strong assumptions and how robust the results are to violations of these assumptions (e.g., independence assumptions, noiseless settings, model well-specification, asymptotic approximations only holding locally). The authors should reflect on how these assumptions might be violated in practice and what the implications would be.
   - The authors should reflect on the scope of the claims made, e.g., if the approach was only tested on a few datasets or with a few runs. In general, empirical results often depend on implicit assumptions, which should be articulated.
   - The authors should reflect on the factors that influence the performance of the approach. For example, a facial recognition algorithm may perform poorly when image resolution is low or images are taken in low lighting. Or a speech-to-text system might not be used reliably to provide closed captions for online lectures because it fails to handle technical jargon.
   - The authors should discuss the computational efficiency of the proposed algorithms and how they scale with dataset size.
   - If applicable, the authors should discuss possible limitations of their approach to address problems of privacy and fairness.
   - While the authors might fear that complete honesty about limitations might be used by reviewers as grounds for rejection, a worse outcome might be that reviewers discover limitations that aren't acknowledged in the paper. The authors should use their best judgment and recognize that individual actions in favor of transparency play an important role in developing norms that preserve the integrity of the community. Reviewers will be specifically instructed to not penalize honesty concerning limitations.

3. **Theory assumptions and proofs**

   Question: For each theoretical result, does the paper provide the full set of assumptions and a complete (and correct) proof?

   Answer: [Yes]

Justification: The full set of assumptions and complete proofs are provided in Appendix D.

Guidelines:

- The answer NA means that the paper does not include theoretical results.
- All the theorems, formulas, and proofs in the paper should be numbered and cross-referenced.
- All assumptions should be clearly stated or referenced in the statement of any theorems.
- The proofs can either appear in the main paper or the supplemental material, but if they appear in the supplemental material, the authors are encouraged to provide a short proof sketch to provide intuition.
- Inversely, any informal proof provided in the core of the paper should be complemented by formal proofs provided in appendix or supplemental material.
- Theorems and Lemmas that the proof relies upon should be properly referenced.

4. **Experimental result reproducibility**

   Question: Does the paper fully disclose all the information needed to reproduce the main experimental results of the paper to the extent that it affects the main claims and/or conclusions of the paper (regardless of whether the code and data are provided or not)?

   Answer: [Yes]

   Justification: We explained our settings in Section 5.1 and hyperparameters in Appendix F.

   Guidelines:

   - The answer NA means that the paper does not include experiments.
   - If the paper includes experiments, a No answer to this question will not be perceived well by the reviewers: Making the paper reproducible is important, regardless of whether the code and data are provided or not.
   - If the contribution is a dataset and/or model, the authors should describe the steps taken to make their results reproducible or verifiable.
   - Depending on the contribution, reproducibility can be accomplished in various ways. For example, if the contribution is a novel architecture, describing the architecture fully might suffice, or if the contribution is a specific model and empirical evaluation, it may be necessary to either make it possible for others to replicate the model with the same dataset, or provide access to the model. In general. releasing code and data is often one good way to accomplish this, but reproducibility can also be provided via detailed instructions for how to replicate the results, access to a hosted model (e.g., in the case of a large language model), releasing of a model checkpoint, or other means that are appropriate to the research performed.
   - While NeurIPS does not require releasing code, the conference does require all submissions to provide some reasonable avenue for reproducibility, which may depend on the nature of the contribution. For example
     (a) If the contribution is primarily a new algorithm, the paper should make it clear how to reproduce that algorithm.
     (b) If the contribution is primarily a new model architecture, the paper should describe the architecture clearly and fully.
     (c) If the contribution is a new model (e.g., a large language model), then there should either be a way to access this model for reproducing the results or a way to reproduce the model (e.g., with an open-source dataset or instructions for how to construct the dataset).
     (d) We recognize that reproducibility may be tricky in some cases, in which case authors are welcome to describe the particular way they provide for reproducibility. In the case of closed-source models, it may be that access to the model is limited in some way (e.g., to registered users), but it should be possible for other researchers to have some path to reproducing or verifying the results.

5. **Open access to data and code**

   Question: Does the paper provide open access to the data and code, with sufficient instructions to faithfully reproduce the main experimental results, as described in supplemental material?

Answer: [No]

Justification: Our experiments use only open-source datasets, while the code required to reproduce these findings does not shared at this time.

Guidelines:

- The answer NA means that paper does not include experiments requiring code.
- Please see the NeurIPS code and data submission guidelines (`https://nips.cc/public/guides/CodeSubmissionPolicy`) for more details.
- While we encourage the release of code and data, we understand that this might not be possible, so "No" is an acceptable answer. Papers cannot be rejected simply for not including code, unless this is central to the contribution (e.g., for a new open-source benchmark).
- The instructions should contain the exact command and environment needed to run to reproduce the results. See the NeurIPS code and data submission guidelines (`https://nips.cc/public/guides/CodeSubmissionPolicy`) for more details.
- The authors should provide instructions on data access and preparation, including how to access the raw data, preprocessed data, intermediate data, and generated data, etc.
- The authors should provide scripts to reproduce all experimental results for the new proposed method and baselines. If only a subset of experiments are reproducible, they should state which ones are omitted from the script and why.
- At submission time, to preserve anonymity, the authors should release anonymized versions (if applicable).
- Providing as much information as possible in supplemental material (appended to the paper) is recommended, but including URLs to data and code is permitted.

6. **Experimental setting/details**

   Question: Does the paper specify all the training and test details (e.g., data splits, hyperparameters, how they were chosen, type of optimizer, etc.) necessary to understand the results?

   Answer: [Yes]

   Justification: The training and test details are presented in Section 5 and Appendix F.

   Guidelines:

   - The answer NA means that the paper does not include experiments.
   - The experimental setting should be presented in the core of the paper to a level of detail that is necessary to appreciate the results and make sense of them.
   - The full details can be provided either with the code, in appendix, or as supplemental material.

7. **Experiment statistical significance**

   Question: Does the paper report error bars suitably and correctly defined or other appropriate information about the statistical significance of the experiments?

   Answer: [No]

   Justification: The experiments are expensive to run for a sufficient number of times to provide error bars at this point.

   Guidelines:

   - The answer NA means that the paper does not include experiments.
   - The authors should answer "Yes" if the results are accompanied by error bars, confidence intervals, or statistical significance tests, at least for the experiments that support the main claims of the paper.
   - The factors of variability that the error bars are capturing should be clearly stated (for example, train/test split, initialization, random drawing of some parameter, or overall run with given experimental conditions).
   - The method for calculating the error bars should be explained (closed form formula, call to a library function, bootstrap, etc.)
   - The assumptions made should be given (e.g., Normally distributed errors).

- It should be clear whether the error bar is the standard deviation or the standard error of the mean.
- It is OK to report 1-sigma error bars, but one should state it. The authors should preferably report a 2-sigma error bar than state that they have a 96% CI, if the hypothesis of Normality of errors is not verified.
- For asymmetric distributions, the authors should be careful not to show in tables or figures symmetric error bars that would yield results that are out of range (e.g. negative error rates).
- If error bars are reported in tables or plots, The authors should explain in the text how they were calculated and reference the corresponding figures or tables in the text.

8. **Experiments compute resources**

   Question: For each experiment, does the paper provide sufficient information on the computer resources (type of compute workers, memory, time of execution) needed to reproduce the experiments?

   Answer: [Yes]

   Justification: The information on the computer resources is reported in Appendix F.

   Guidelines:

   - The answer NA means that the paper does not include experiments.
   - The paper should indicate the type of compute workers CPU or GPU, internal cluster, or cloud provider, including relevant memory and storage.
   - The paper should provide the amount of compute required for each of the individual experimental runs as well as estimate the total compute.
   - The paper should disclose whether the full research project required more compute than the experiments reported in the paper (e.g., preliminary or failed experiments that didn't make it into the paper).

9. **Code of ethics**

   Question: Does the research conducted in the paper conform, in every respect, with the NeurIPS Code of Ethics `https://neurips.cc/public/EthicsGuidelines`?

   Answer: [Yes]

   Justification: The research conducted in the paper conform, in every respect, with the NeurIPS Code of Ethics.

   Guidelines:

   - The answer NA means that the authors have not reviewed the NeurIPS Code of Ethics.
   - If the authors answer No, they should explain the special circumstances that require a deviation from the Code of Ethics.
   - The authors should make sure to preserve anonymity (e.g., if there is a special consideration due to laws or regulations in their jurisdiction).

10. **Broader impacts**

    Question: Does the paper discuss both potential positive societal impacts and negative societal impacts of the work performed?

    Answer: [Yes]

    Justification: The potential societal impacts of this work are discussed in Section 1 and Section 2.

    Guidelines:

    - The answer NA means that there is no societal impact of the work performed.
    - If the authors answer NA or No, they should explain why their work has no societal impact or why the paper does not address societal impact.
    - Examples of negative societal impacts include potential malicious or unintended uses (e.g., disinformation, generating fake profiles, surveillance), fairness considerations (e.g., deployment of technologies that could make decisions that unfairly impact specific groups), privacy considerations, and security considerations.

- The conference expects that many papers will be foundational research and not tied to particular applications, let alone deployments. However, if there is a direct path to any negative applications, the authors should point it out. For example, it is legitimate to point out that an improvement in the quality of generative models could be used to generate deepfakes for disinformation. On the other hand, it is not needed to point out that a generic algorithm for optimizing neural networks could enable people to train models that generate Deepfakes faster.
- The authors should consider possible harms that could arise when the technology is being used as intended and functioning correctly, harms that could arise when the technology is being used as intended but gives incorrect results, and harms following from (intentional or unintentional) misuse of the technology.
- If there are negative societal impacts, the authors could also discuss possible mitigation strategies (e.g., gated release of models, providing defenses in addition to attacks, mechanisms for monitoring misuse, mechanisms to monitor how a system learns from feedback over time, improving the efficiency and accessibility of ML).

11. **Safeguards**

    Question: Does the paper describe safeguards that have been put in place for responsible release of data or models that have a high risk for misuse (e.g., pretrained language models, image generators, or scraped datasets)?

    Answer: [NA]

    Justification: This paper poses no such risks.

    Guidelines:

    - The answer NA means that the paper poses no such risks.
    - Released models that have a high risk for misuse or dual-use should be released with necessary safeguards to allow for controlled use of the model, for example by requiring that users adhere to usage guidelines or restrictions to access the model or implementing safety filters.
    - Datasets that have been scraped from the Internet could pose safety risks. The authors should describe how they avoided releasing unsafe images.
    - We recognize that providing effective safeguards is challenging, and many papers do not require this, but we encourage authors to take this into account and make a best faith effort.

12. **Licenses for existing assets**

    Question: Are the creators or original owners of assets (e.g., code, data, models), used in the paper, properly credited and are the license and terms of use explicitly mentioned and properly respected?

    Answer: [NA]

    Justification: We did not use existing assets.

    Guidelines:

    - The answer NA means that the paper does not use existing assets.
    - The authors should cite the original paper that produced the code package or dataset.
    - The authors should state which version of the asset is used and, if possible, include a URL.
    - The name of the license (e.g., CC-BY 4.0) should be included for each asset.
    - For scraped data from a particular source (e.g., website), the copyright and terms of service of that source should be provided.
    - If assets are released, the license, copyright information, and terms of use in the package should be provided. For popular datasets, `paperswithcode.com/datasets` has curated licenses for some datasets. Their licensing guide can help determine the license of a dataset.
    - For existing datasets that are re-packaged, both the original license and the license of the derived asset (if it has changed) should be provided.

- If this information is not available online, the authors are encouraged to reach out to the asset's creators.

13. **New assets**

    Question: Are new assets introduced in the paper well documented and is the documentation provided alongside the assets?

    Answer: [NA]

    Justification: This paper does not release new assets.

    Guidelines:

    - The answer NA means that the paper does not release new assets.
    - Researchers should communicate the details of the dataset/code/model as part of their submissions via structured templates. This includes details about training, license, limitations, etc.
    - The paper should discuss whether and how consent was obtained from people whose asset is used.
    - At submission time, remember to anonymize your assets (if applicable). You can either create an anonymized URL or include an anonymized zip file.

14. **Crowdsourcing and research with human subjects**

    Question: For crowdsourcing experiments and research with human subjects, does the paper include the full text of instructions given to participants and screenshots, if applicable, as well as details about compensation (if any)?

    Answer: [NA]

    Justification: This paper dose not involve crowdsourcing nor research with human subjects.

    Guidelines:

    - The answer NA means that the paper does not involve crowdsourcing nor research with human subjects.
    - Including this information in the supplemental material is fine, but if the main contribution of the paper involves human subjects, then as much detail as possible should be included in the main paper.
    - According to the NeurIPS Code of Ethics, workers involved in data collection, curation, or other labor should be paid at least the minimum wage in the country of the data collector.

15. **Institutional review board (IRB) approvals or equivalent for research with human subjects**

    Question: Does the paper describe potential risks incurred by study participants, whether such risks were disclosed to the subjects, and whether Institutional Review Board (IRB) approvals (or an equivalent approval/review based on the requirements of your country or institution) were obtained?

    Answer: [NA]

    Justification: This paper dose not involve crowdsourcing nor research with human subjects.

    Guidelines:

    - The answer NA means that the paper does not involve crowdsourcing nor research with human subjects.
    - Depending on the country in which research is conducted, IRB approval (or equivalent) may be required for any human subjects research. If you obtained IRB approval, you should clearly state this in the paper.
    - We recognize that the procedures for this may vary significantly between institutions and locations, and we expect authors to adhere to the NeurIPS Code of Ethics and the guidelines for their institution.
    - For initial submissions, do not include any information that would break anonymity (if applicable), such as the institution conducting the review.

16. **Declaration of LLM usage**

Question: Does the paper describe the usage of LLMs if it is an important, original, or non-standard component of the core methods in this research? Note that if the LLM is used only for writing, editing, or formatting purposes and does not impact the core methodology, scientific rigorousness, or originality of the research, declaration is not required.

Answer: [NA]

Justification: LLMs were used for minor language editing, which does not affect the scientific contribution of the paper.

Guidelines:

- The answer NA means that the core method development in this research does not involve LLMs as any important, original, or non-standard components.
- Please refer to our LLM policy (`https://neurips.cc/Conferences/2025/LLM`) for what should or should not be described.

A Comparative Analysis of Neighborhood Structures

The critical path, whose length represents the makespan $C_{\max}$, is essential in constructing feasible solutions [55]. Operations on this path are critical operations, and critical blocks are maximal sequences of adjacent critical operations processed on the same machine [45]. In local search, the neighborhood comprises feasible solutions generated by small perturbations to the current one [55]. For scheduling, these perturbations typically involve reordering operations on the critical path. The neighborhood structure directly affects the efficiency of the search algorithm, making it important to eliminate unnecessary or infeasible moves [45]. Among various neighborhood designs, the N5 neighborhood is significantly smaller than others [45]. It identifies a single critical path and defines a move by reversing either the first two or the last two operations within a critical block.

While effective for JSP [21], the N5 neighborhood cannot be applied to FJSP. Its limitation lies in only permitting reordering within one critical block, where operations are processed on the same machine. This perturbation preserves the original machine assignments, severely constraining the exploration of the solution space. More critically, unlike JSP where operations of the same job are processed on different machines, FJSP allows multiple operations of a job to be processed on the same one. Consequently, swapping operations within critical blocks in FJSP may violate job precedence constraints, resulting in infeasible solutions (Figure 5).

In contrast, we employ the Nopt2 neighborhood [51] that simultaneously modifies operation sequences and machine assignments while maintaining feasibility through time-constrained reinsertion (see paragraph 3). This structure enables broader solution space exploration and improves efficiency by using optimal insertion intervals to reduce the neighborhood size.

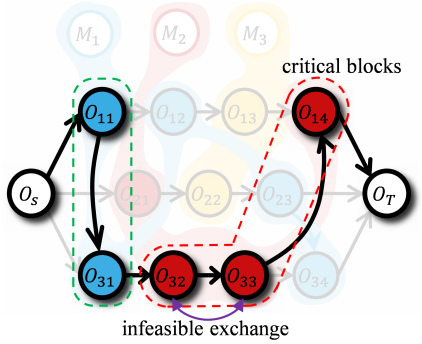

Figure 5 **Infeasible exchange caused by the N5 neighborhood in FJSP.** Dotted lines of different colors are critical blocks.

B Definition of Raw Feature Vectors

The raw features of operations and machines at each state s_t (omitting step t) are defined as follows. *Features of Operations*: Each operation node $O_{ij} \in \mathcal{O} \setminus \{O_S, O_T\}$ is represented by a 9-dimensional feature vector $\mathbf{x}_{O_{ij}}$:

1) **Minimum Processing Time**: shortest processing time among compatible machines.
2) **Average Processing Time**: mean processing time among compatible machines.
3) **Range of Processing Time**: difference between the maximum and minimum processing times among compatible machines.
4) **Machine Availability Ratio**: ratio of the number of compatible machines to total machines.
5) **Processing Time**: processing time on the assigned machine.
6) **Earliest Start Time**: earliest possible start time of the operation.
7) **Latest Start Time**: latest start time without schedule delay.
8) **Scheduling Order on Machine**: execution order on machine M_k (starting from 1).
9) **Processing Time of Job**: total processing time of parent job.

Features of Machines: Each machine node $M_k \in \mathcal{M}$ owns a 4-dimensional feature vector $\mathbf{y}_{M_k}$:

1) **Utilization Rate**: ratio of active processing time to makespan.

2) **Criticality Degree**: proportion of operations on critical path among processable operations.
3) **Load Ratio**: percentage of assigned operations versus machine capacity.
4) **Processing Efficiency**: mean processing time of assigned operations.

C Advantages of the Directed Heterogeneous Graph

In the FJSP, the global scheduling state comprises both operations and machines. However, the absence of machine nodes in traditional disjunctive graphs results in an indirect representation of machine information through numerical values [21], which limits the policy from assigning operations to available machines effectively. The heterogeneous disjunctive graph $\mathcal{H}$ [8] addresses this by introducing machine nodes (Fig. 6), where each operation connects to compatible machines via undirected edges, such that solving the FJSP is equivalent to selecting one O-M arc per operation while removing others. This reduces the graph density from $\sum_{k=1}^{|\mathcal{M}|}\binom{n_k}{2}$ to $\sum_{k=1}^{|\mathcal{M}|} n_k$ with n_k being the number of operations assignable to machine M_k and enables better injection of machine status [8].

While beneficial for construction methods, this structure provides limited advantages for improvement approaches where complete solutions contain fixed machine assignments. This leads to a total of $|\mathcal{O}|$ disjunctive arcs—more than the $|\mathcal{O}| - |\mathcal{M}|$ arcs in the conventional graph, negating the benefit of reduced graph density. Most importantly, undirected edges hinder the clear encoding of machine processing sequences, which is crucial for distinguishing between different scheduling solutions and identifying the critical path when constructing the action space [21, 51]. Instead, our heterogeneous graph $\overrightarrow{\mathcal{H}}$(Figure 1c), tailored for complete schedules, overcomes this limitation by encoding machine processing sequences through directed hyper-edges, which effectively represent the ordering of operations across different solutions without significantly increasing graph density. It adopts a unified structure with fully directed arrows, avoiding the complexity of mixed edge types and better aligning with current learning-to-search graph-based frameworks [21].

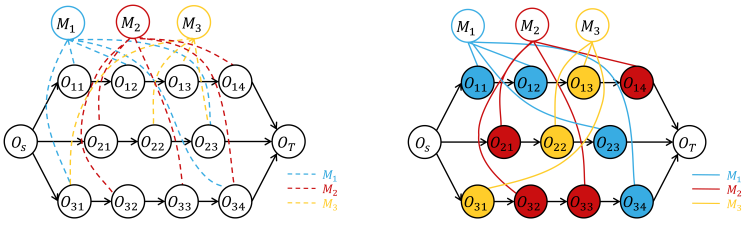

(a) (b)

Figure 6 **Graph representations in $\mathcal{H}$ [8].** (a) FJSP instance; (b) feasible solution.

D Compact State Representation in Memory

D.1 Motivation and Compact Formulation

During the improvement, we store the state-action pair (s_t, a_t) at each step in a memory module. However, the state is represented as a complex heterogeneous graph with rich node attributes and adjacency relations, leading to excessive memory consumption if fully stored. Furthermore, evaluating similarity between such graphs typically requires GNNs to extract embeddings, introducing additional network components and computational cost.

To address this, we simplify the graph representation to better support our memory mechanism. First, since our current goal is to distinguish different scheduling solutions—rather than using node features as heuristic guidance—we omit the node attributes and retain only the graph topology. Second, for a given problem instance, solutions differ only in operation sequences on machines (i.e., hyper-arcs), while sharing the same job precedence constraints (i.e., conjunctive arcs). Based on this insight, we isolate the hyper-arcs from $\overrightarrow{\mathcal{H}}_t$ (see Fig. 7) and use them as the key feature to characterize each solution. Specifically, we use the operation-machine incidence matrix $\boldsymbol{L}_t$ as a compact representation of s_t and measure similarity via the Frobenius inner product.

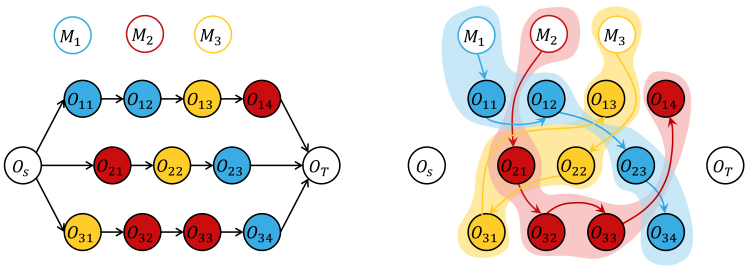

(a) (b)

Figure 7 **Decomposition of FJSP solution structure.** (a) shared job precedence constraints; (b) distinct machine processing sequences.

Instead of serving as merely binary indicators of machine assignment, the non-zero element $(\boldsymbol{L}_t)_{i,j}$ represents the processing order index of operation i on its assigned machine j. This crucial design ensures that two schedules with identical machine assignments but different sequences (e.g., a good sequence vs. a poor one) are correctly distinguished. For instance, a good sequence of operations corresponding to [*1, 2, 3, 4, 5*] and a poor, reversed sequence [*5, 4, 3, 2, 1*] on the same machine will be recognized as maximally dissimilar by the Frobenius inner product. The mathematical foundation for this lies in the **Rearrangement Inequality**, which guarantees that the inner product is maximized for similarly ordered sequences and minimized for oppositely ordered ones. This allows our similarity metric to be both computationally efficient and highly sensitive to the quality of the operation sequence.

Theorem 1. *The Rearrangement Inequality states that, for two sequences* $a_1 \leq a_2 \leq \cdots \leq a_n$ *and* $b_1 \leq b_2 \leq \cdots \leq b_n$*, the inequalities*

$$a_1 b_n + a_2 b_{n-1} + \cdots + a_n b_1 \leq a_1 b_{\pi(1)} + a_2 b_{\pi(2)} + \cdots + a_n b_{\pi(n)} \leq a_1 b_1 + a_2 b_2 + \cdots + a_n b_n$$

hold, where $\pi(1), \pi(2), \ldots, \pi(n)$ *is any permutation of* $1, 2, \ldots, n$*.*

D.2 Alternative Designs

We have considered and tested other expressive representations for the historical states that explicitly encode sequence information.

Multi matrices: The adjacency matrix A_t^M of operations on machines encodes the processing order between operations, while the binary operation-machine incidence matrix L_t^B indicates machine assignment. The state similarity is then calculated by computing the inner products of both matrices separately and summing the results, expressed as:

$$\omega_{t,t'} = \langle L_t^B, L_{t'}^B \rangle_F + \langle A_t^M, A_{t'}^M \rangle_F \tag{8}$$

Difference matrix: For the operation-machine incidence matrices that store processing order indices, we compute the element-wise difference between two schedules, L_t and $L_{t'}$, to obtain a difference matrix, and then use the reciprocal of its Frobenius norm to measure similarity, formulated as:

$$\omega_{t,t'} = \frac{1}{|L_t - L_{t'}|_F + \epsilon} = \frac{1}{\sqrt{\sum_{i=1}^{|\mathcal{O}|} \sum_{j=1}^{|\mathcal{M}|} |(L_t)_{i,j} - (L_{t'})_{i,j}|^2} + \epsilon} \tag{9}$$

However, these alternatives introduced higher storage or computational overhead without yielding significant performance gains. Our chosen representation thus strikes a deliberate and effective balance between representational power and efficiency.

E Complexity Analysis of Action Space

Let $F_O \in \mathbb{R}^{|\mathcal{O}| \times q}$ and $F_M \in \mathbb{R}^{|\mathcal{M}| \times q}$ denote the embedding matrices of operation and machine nodes, respectively. To assign a priority score to each possible triple-action $[O_m, O_n, M_k]$, we compute the priority matrix $F_{OOM} \in \mathbb{R}^{|\mathcal{O}| \times |\mathcal{O}| \times |\mathcal{M}|}$ through a two-step tensor operations involving F_O and F_M. As a result, the space complexity of the action space $\mathcal{A}_{original}$ is $O(|\mathcal{O}|^2 |\mathcal{M}|)$. Prior

work [60] has shown that a large number of possible actions is known to lead to over-optimistic estimates of future rewards, degrading agent performance and learning efficiency. To address this, we reshape the action space by exploiting the constraint of FJSP: each operation can only be assigned to a unique machine. Given a solution of FJSP, there exists a mapping $f_M : \mathcal{O} \to \mathcal{M}$, which allows us to omit the third dimension and represent actions as pairs $[O_m, O_n]$. The space complexity of $\mathcal{A}_{optimized}$ is reduced to $O(|\mathcal{O}|^2)$ and the optimized priority matrix is calculated as follows:

$$F_{OO} = F_O F_O^\top \in \mathbb{R}^{|\mathcal{O}|\times|\mathcal{O}|} \tag{10}$$

We can formalize the relationship between the original and optimized action spaces as follows:

Theorem 2. *The optimized action space $\mathcal{A}_{optimized}$ is functionally equivalent to $\mathcal{A}_{original}$ in terms of admissible actions under the FJSP constraints.*

Proof. For any feasible action $a = [O_m, O_n, M_k] \in \mathcal{A}_{original}$, there exists a unique $a' = [O_m, O_n] \in \mathcal{A}_{optimized}$ with $M_k = f_M(O_n)$. Conversely, any $a' \in \mathcal{A}_{optimized}$ can be mapped back to $a \in \mathcal{A}_{original}$ via f_M. Thus, this compaction preserves all feasible actions while eliminating invalid ones (i.e., actions where the operation and machine do not match). This shaping of the action space reduces learning difficulty and accelerates model convergence without compromising the agent's performance. □

Algorithm 1: Training procedure with n-step PPO using parallel search.

Input: *MIStar* with trainable parameters $\Theta = \{\delta, \theta, \varphi\}$, parallel scale P, iteration limit T, update size n, validate size v, new data generation step d, batch size B, total number of training epochs I;

Output: Trained *MIStar* with parameters $\Theta^* = \{\delta^*, \theta^*, \varphi^*\}$;

for $i = 0$ **to** $i < I$ **do**
  if $i \bmod d = 0$ **then**
    Randomly generate B instances;
  end
  Compute initial solutions $\{s_0^1, \ldots, s_0^B\}$ using DANIEL;
  for $t = 0$ **to** T **do**
    for $s_t^b \in \{s_t^1, \ldots, s_t^B\}$ **do**
      Initialize a training data buffer D^b and memory buffer H^b with size 0;
      Extract embeddings using MHGNN;
      for $p = 1$ **to** P **do**
        Sample a local move $a_t^{bp} \sim \pi_\delta(\cdot|s_t^b)$;
        Compute $C_{\max}(s_{t+1}^{bp})$ w.r.t a_t^{bp};
      end
      Identify the best action a_t^{b*} with greatest improvement ;
      Update s_t^b w.r.t a_t^{b*} and compute similarity score Ω from H^b;
      Compute reward $r_t(s_t^b, a_t^{b*}) = r_{gain} - r_{penalty}$;
      Store the data (s_t^b, a_t^{b*}, r_t) into D^b and store (s_t^b, a_t^{b*}) into H^b;
      if $t \bmod n = 0$ **then**
        Compute the generalised advantage estimates $\hat{A}_t$;
        Compute the PPO loss L, and optimize the parameters Θ for R epochs;
        Update network parameters;
      end
      Clear buffers D^b and H^b;
    end
  end
  if $i \bmod v = 0$ **then**
    Validate the policy;
  end
  $i = i + B$;
end

F The n-step PPO Algorithm with Parallel Greedy Exploration Strategy

We adopt the PPO algorithm [61] based on the actor-critic architecture as our training strategy. The actor is the policy network and the critic provides state value estimation. The network parameters are updated every n steps, which effectively addresses sparse rewards and out-of-memory issues [21]. The flexibility of FJSP leads to a large solution space, requiring numerous iterations to converge to high-quality solutions [30]. To address this challenge, we introduce a parallel greedy exploration strategy, which evaluates multiple candidate actions in parallel and greedily selects the one yielding the greatest improvement. This approach enables the exploration of multiple solutions per iteration, yielding high-quality results with fewer iterations. Moreover, by prioritizing solutions with the greatest improvement, the model is guided toward more promising paths, minimizing the interference from inefficient paths during gradient updates and accelerating convergence.

The pseudo-code of the n-step PPO algorithm is presented in Algorithm 1.

G Training Configurations

All hyperparameters were fine-tuned on the smallest-scale instances from SD2 and kept the same for all other models. Experiments were conducted on a platform equipped with an Intel i9-12900K processor with 24 cores, 64 GB memory, and an NVIDIA RTX 4090 GPU with 24 GB VRAM. Detailed specifications are provided in Table 5. Upon acceptance of this manuscript for publication, the full code will be made available on GitHub.

Table 5 Training configuration parameters

Parameter	Value
Number of MHGNN layers (L)	4
Number of Actor network layers	4
Number of Critic network layers	3
Number of attention heads in GAT (n_H)	1
Dimension of hidden layers (q)	64
GIN learnable parameter (ϵ)	0
Discount factor (γ)	1
Clipping ratio	0.2
Policy function coefficient	1
Value function coefficient	0.5
Entropy coefficient	0.01
Learning rate	5×10^{-4}
Optimizer	Adam
Memory buffer size	600
KNN retrieval count (K)	15
Similarity penalty coefficient (λ)	10
PPO update interval (n)	10
Rounds per PPO update (R)	3
Total training epochs (I)	20,000
Validation interval (v)	5
Instance generation interval (d)	20
Iterations per instance (T)	100
Batch size (B)	20
Parallel scale (P)	50

H Detailed Analysis on Synthetic Instances

Our experiments on four small-sized instances from SD2 reveal that *MIStar* generates an action space consisting of dozens to hundreds of possible moves per iteration using the Nopt2 neighborhood—up to 100 times larger than [21] for solving JSP. While this expanded action space provides greater

Table 6 Results of different initialization methods

Method	Iter.	SD2							
		10×5		20×5		15×10		20×10	
		Obj.	Gap	Obj.	Gap	Obj.	Gap	Obj.	Gap
DANIEL(S)	0	365.26	0.00%	629.56	0.00%	522.51	0.00%	552.38	0.00%
	100	345.05	5.53%	615.12	2.29%	488.22	6.56%	530.93	3.88%
	200	343.43	5.98%	613.75	2.51%	476.93	8.72%	528.92	4.25%
	400	**342.50**	6.23%	**612.73**	2.67%	**465.71**	10.87%	**525.49**	4.87%
HGNN(S)	0	479.35	0.00%	963.03	0.00%	759.54	0.00%	984.64	0.00%
	100	375.20	21.73%	745.18	22.62%	677.96	10.74%	879.48	10.68%
	200	366.35	23.57%	702.90	27.01%	626.90	17.46%	812.53	17.48%
	400	359.10	25.09%	674.93	29.92%	569.81	24.98%	737.42	25.11%
SPT	0	503.86	0.00%	799.56	0.00%	670.56	0.00%	775.03	0.00%
	100	399.25	20.76%	692.43	13.40%	578.48	13.73%	695.34	10.28%
	200	393.74	21.86%	680.62	14.88%	550.94	17.84%	673.44	13.11%
	400	389.34	22.73%	671.05	16.07%	521.96	22.16%	648.48	16.33%
MWKR	0	493.36	0.00%	949.85	0.00%	737.44	0.00%	953.11	0.00%
	100	382.09	22.55%	747.12	21.34%	664.69	9.87%	858.45	9.93%
	200	372.62	24.47%	705.15	25.76%	618.86	16.08%	799.61	16.11%
	400	364.99	26.02%	676.88	28.74%	563.56	23.58%	729.91	23.42%
FIFO	0	476.96	0.00%	931.50	0.00%	763.12	0.00%	978.03	0.00%
	100	376.29	21.11%	729.85	21.65%	669.51	12.27%	861.06	11.96%
	200	367.70	22.91%	693.35	25.57%	618.74	18.92%	799.15	18.29%
	400	360.68	24.38%	668.26	28.26%	562.59	26.28%	728.91	25.47%
RANDOM	0	585.08	0.00%	1067.38	0.00%	1062.39	0.00%	1304.70	0.00%
	100	382.24	34.67%	750.69	29.67%	733.17	30.99%	960.68	26.37%
	200	371.38	36.52%	707.33	33.73%	661.03	37.78%	865.85	33.64%
	400	365.33	**37.56%**	678.00	**36.48%**	589.53	**44.51%**	772.15	**40.82%**

optimization potential, it also introduces more suboptimal solutions, increasing the risk of local optima entrapment. Moreover, even for small-sized problems, OR-Tools could only optimally solve a small portion of instances within the time limit [22]. These observations underscore the complexity of the FJSP. Compared with rule-based improvement heuristics, *MIStar* shows superior performance under the same iteration budget, with only a marginal shortfall (0.06%) against the BI rule on the SD2 40×10 instance at 100 iterations. Notably, even equipped with *restart*, rule-based methods still tend to stagnate as iterations increase—likely due to the large and complex solution space—whereas *MIStar* continues to improve, demonstrating the effectiveness of the learned policy. Additionally, *MIStar* reduces runtime by directly outputting local moves, avoiding exhaustive evaluations across the entire neighborhood.

I Improvement over Varied Initial Solution Generation Methods

We systematically evaluate the optimization capabilities of *MIStar* using six initialization strategies: two DRL-based construction methods with sampling (DANIEL(S) and HGNN(S)), random initialization, and three classical priority dispatching rules—shortest processing time (SPT), most work remaining (MWKR), and first-in-first-out (FIFO) [55]. Experiments are conducted on the SD2 dataset with models trained on instances of the same size, to assess the performance across different initialization methods under the fixed iteration budget. Improvement is measured by the makespan gap, calculated as $\left(1 - \frac{C_{\text{best}}}{C_0}\right) \times 100\%$, where C_0 is the makespan of the initial solution and C_{best} is the incumbent optimal value.

The results are detailed in Table 6. It can be observed that the quality of initial solutions impacts the search efficiency of *MIStar*. With the same number of iterations, better initial solutions enable *MIStar* to generate higher-quality schedules, while poorer ones typically allow for larger relative improvements. Notably, after 400 iterations, solutions initialized by HGNN(S), MWKR, and FIFO outperform those generated by DANIEL(S) with 0 iteration on the 10×5 instances. This demonstrates that, with a sufficient iteration budget, *MIStar* has the potential to elevate weaker initial solutions to a performance level comparable to that of stronger ones. Moreover, even when starting from (near)-optimal solutions initialized by DANIEL(S), *MIStar* still achieves notable improvements, further validating the effectiveness of our framework.

Table 7 Performance of ablated models

Model	Iter.	SD2							
		10×5		20×5		15×10		20×10	
		Obj.	Time[1]	Obj.	Time	Obj.	Time	Obj.	Time
Baseline	100	364.27	0.76s	629.09	1.16s	519.34	1.82s	552.46	2.37s
	200	364.27	1.48s	629.09	2.44s	519.34	3.69s	552.46	4.78s
	400	364.27	2.89s	629.09	4.85s	519.34	7.25s	552.46	9.48s
w/o GIN	100	348.31	4.97s	616.71	10.72s	491.78	18.12s	548.61	24.80s
	200	347.06	10.78s	614.98	22.88s	484.36	37.58s	545.97	53.68s
	400	345.73	20.56s	613.98	45.90s	477.80	1.45m	544.31	1.91m
w/o GAT	100	350.86	5.82s	618.67	11.34s	492.76	17.85s	548.0	22.63s
	200	349.89	9.46s	617.33	22.91s	486.74	36.97s	547.97	51.02s
	400	348.33	21.41s	615.99	46.79s	480.66	1.29m	547.87	1.78m
w/o HGAT	100	350.49	5.44s	618.15	11.39s	491.97	17.95s	535.78	23.89s
	200	349.08	9.74s	616.56	23.01s	483.46	37.01s	532.83	52.47s
	400	347.17	20.10s	614.97	46.38s	473.83	1.29m	529.92	1.67m
w/o Par.	100	363.02	0.59s	627.20	0.98s	518.28	1.68s	551.39	2.41s
	200	363.02	1.22s	627.20	2.13s	518.28	4.02s	551.39	6.18s
	400	363.02	2.59s	627.20	5.05s	518.28	11.72s	551.39	17.57s
w/o Mem.	100	346.11	5.47s	615.99	13.98s	490.63	17.25s	534.31	25.47s
	200	344.76	11.04s	615.32	25.33s	486.16	35.85s	531.71	51.08s
	400	343.53	20.24s	614.80	48.91s	482.16	73.14s	528.44	1.69m
Ours	100	345.05	5.27s	615.12	11.55s	488.22	18.09s	530.93	25.76s
	200	343.43	10.33s	613.75	23.50s	476.93	37.42s	528.92	53.25s
	400	**342.50**	21.39s	**612.73**	47.93s	**465.71**	1.31m	**525.49**	1.88m

[1] "s" and "m" denote seconds and minutes, respectively.

J Results on Ablation Studies

J.1 Analysis on Components and Strategy

We conducted comprehensive ablation studies to evaluate the contributions of the key components of our framework, including both the model architecture and the search strategy. The experiments were performed on four small-size instances from the SD2 dataset.

We first assessed the roles of the memory module and the parallel greedy search strategy. Three ablated variants are compared: the *Baseline* model without any enhancements, a version without the parallel greedy search strategy (*w/o Par.*), and another without the memory module (*w/o Mem.*). Results in Table 7 demonstrate the critical roles of both components. Although our parallel approach takes longer per iteration, it achieves superior solutions in fewer steps, improving search efficiency. In contrast, the model without parallelism runs faster but consistently converges to inferior local optima. Furthermore, while the memory module helps enhance the decision-making of the policy, it alone (i.e., *w/o Par.*) proves insufficient to escape local optima. This limitation may stem from the fact that the FJSP solution space is extremely large and complex, making it challenging for the policy network to achieve effective global exploration through sparse, single-step sampling. For future work, a critical direction involves dynamically constraining the search space or optimizing the memory mechanism to selectively extract salient historical features.

Our tailored representation module, which is composed of multiple specialized graph encoders, is not only theoretically motivated by the structural characteristics of FJSP graphs but is also aligned with mainstream graph learning practices [8, 21, 24, 50]. The ablation results by removing each component (i.e., *w/o GAT*, *w/o GIN* and *w/o HGAT*) confirm that each of them is essential for learning informative and discriminative state representations that support effective policy learning.

J.2 Evaluation of Search Scale

Using models trained with $P = 50$, we systematically evaluated the search strategy across different parallel scales $P \in \{10, 20, 30, 40, 50, 60, 70\}$ on SD2 instances of two sizes. The result curves are illustrated in Figure 8. It is evident that increasing P leads to longer runtimes under a fixed number of iterations. Moreover, the runtime scales linearly with the iteration count across different P values. Regarding solution quality, the 10×5 instance has a relatively small neighborhood (approximately 80 solutions), making $P = 20$ sufficient to cover most promising moves. Consequently, further increasing P does not yield noticeable improvement. On the other hand, the 15×10 instance has

around 240 neighbors, so increasing P from 10 to 60 continuously improves performance. However, the difference between $P = 60$ and $P = 70$ becomes negligible, indicating a saturation point beyond which additional evaluations offer little benefit. These observations highlight the importance of selecting an appropriate P based on the problem size and the flexibility of alternative machines to balance performance gains and computational cost. In future work, we plan to enable the network to dynamically adapt P according to instance characteristics, reducing manual tuning efforts.

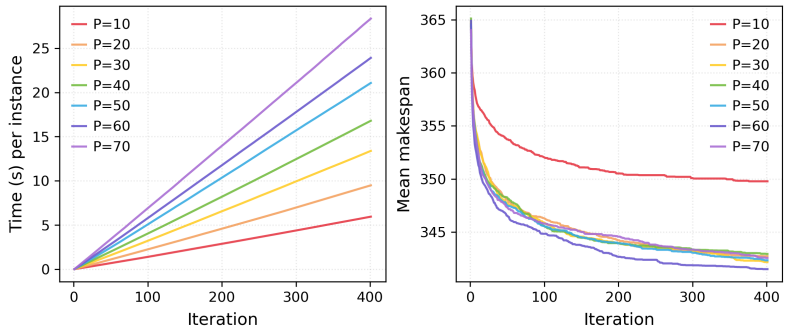

(a) 10×5 instances.

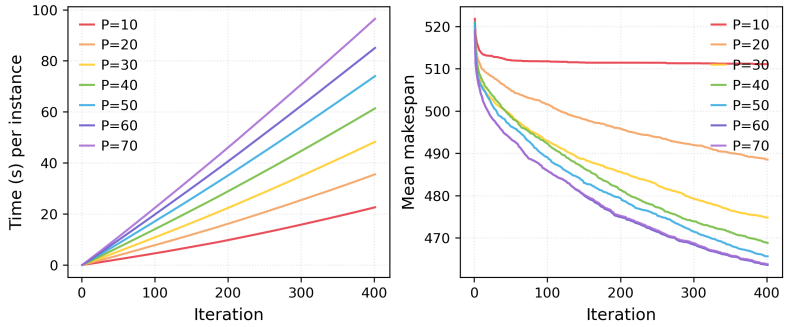

(b) 15×10 instances.

Figure 8 **Runtime (left) and performance (right) curves across different parallel scale.**